

AD-A260 117



2

PL-TR-92-2315

**Lg AND OTHER REGIONAL PHASES IN  
SOUTH AMERICA**

**Ramon Roige Cabre, S.J.  
Estela Ramos Minaya**

**DTIC  
ELECTE  
JAN 29 1993  
S c D**

**Observatorio San Calixto  
Cas. 12656  
La Paz, BOLIVIA**

**October 1992**

10007

**93-01637**



7488

**Final Report  
1 September 1989-31 August 1992**

**APPROVED FOR PUBLIC RELEASE; DISTRIBUTION UNLIMITED**

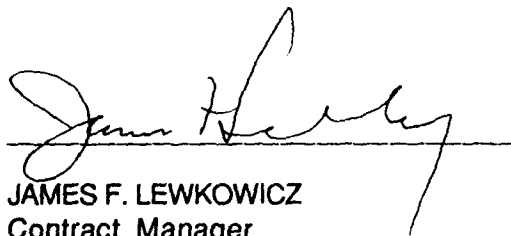


**PHILLIPS LABORATORY  
Directorate of Geophysics  
AIR FORCE MATERIEL COMMAND  
HANSCOM AIR FORCE BASE, MA 01731-5000**

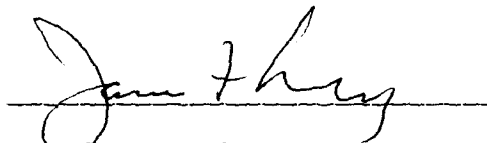
**98 1 28 037**

The views and conclusions contained in this document are those of the authors and should not be interpreted as representing the official policies, either expressed or implied, of the Air Force or the U.S. Government.

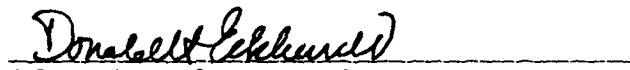
This technical report has been reviewed and is approved for publication.



JAMES F. LEWKOWICZ  
Contract Manager  
Solid Earth Geophysics Branch  
Earth Sciences Division



JAMES F. LEWKOWICZ  
Branch Chief  
Solid Earth Geophysics Branch  
Earth Sciences Division

  
DONALD H. ECKHARDT, Director  
Earth Sciences Division

This document has been reviewed by the ESD Public Affairs Office (PA) and is releasable to the National Technical Information Service (NTIS).

Qualified requestors may obtain additional copies from the Defense Technical Information Center. All others should apply to the National Technical Information Service.

If your address has changed, or if you wish to be removed from the mailing list, or if the addressee is no longer employed by your organization, please notify PL/IMA, Hanscom AFB MA 01731-5000. This will assist us in maintaining a current mailing list.

Do not return copies of this report unless contractual obligations or notices on a specific document requires that it be returned.

## REPORT DOCUMENTATION PAGE

Form Approved  
OMB No. 0704-0188

Public reporting burden for this collection of information is estimated to average 1 hour per response, including the time for reviewing instructions, searching existing data sources, gathering and maintaining the data needed, and completing and reviewing the collection of information. Send comments regarding this burden estimate or any other aspect of this collection of information, including suggestions for reducing this burden, to Washington Headquarters Services, Directorate for Information Operations and Reports, 1215 Jefferson Davis Highway, Suite 1204, Arlington, VA 22202-4302, and to the Office of Management and Budget, Paperwork Reduction Project (0704-0188), Washington, DC 20503.

1. AGENCY USE ONLY (Leave blank)		2. REPORT DATE October 1992	3. REPORT TYPE AND DATES COVERED Final (1 Sep 1989-31 Aug 1992)	
4. TITLE AND SUBTITLE Lg and Other Regional Phases in South America			5. FUNDING NUMBERS PE 61102F PR 9A10 TA DA WU AX  Contract AFOSR-89-0532	
6. AUTHOR(S) Ramon Roige Cabre, S.J. Estela Ramos Minaya				
7. PERFORMING ORGANIZATION NAME(S) AND ADDRESS(ES) Observatorio San Calixto Cas. 12656 La Paz, BOLIVIA			8. PERFORMING ORGANIZATION REPORT NUMBER	
9. SPONSORING / MONITORING AGENCY NAME(S) AND ADDRESS(ES) Phillips Laboratory Hanscom AFB, MA 01731-5000  Contract Manager: James Lewkowicz/GPEH			10. SPONSORING / MONITORING AGENCY REPORT NUMBER  PL-TR-92-2315	
11. SUPPLEMENTARY NOTES				
12a. DISTRIBUTION / AVAILABILITY STATEMENT  APPROVED FOR PUBLIC RELEASE; DISTRIBUTION UNLIMITED			12b. DISTRIBUTION CODE	
13. ABSTRACT (Maximum 200 words) For South American epicenters south of 47°S, no Lg is recorded at LPB. Brazilian earthquakes have a ratio of amplitudes Lg/P $5.2 \pm 0.3$ . Rg is larger: Lg/Rg $0.7 \pm 0.3$ . For the measurement of magnitudes mbLg, the southernmost South America is excluded. The following formulas are adopted: mbLg = $3.80 + 2.00 \log + \log(A/T)$ for cordilleran epicenters and mbLg = $4.40 + 1.15 \log + \log(A/T)$ for shield epicenters (Appendix 1). Rg waves are very small from off the western coast, fair from the coast, clear from continental Peru and largest from southern Peru. Li are shear waves emerging among scattered waves. Preliminary values of Q across Peru and beneath LPB were obtained for P waves and short period guided waves. The intensity attenuation of the nine Bolivian seismogenic zones can be reduced to four values (Appendix 2). Positive P residuals average 2.6 s for oceanic earthquakes and 2.5 for continental ones. Particle motion, spectral analysis and wave recording envelope have been analyzed, but no solid conclusions have been reached for a region so large and diversified. Several hypotheses are presented. In the P-coda, besides pP, other phases originate by scattering, reflection, channelling, caused by subducted Nazca plate and by crustal thickening of the Andes roots. Appendices 3 and 4 expand the analysis of P type phases.				
14. SUBJECT TERMS South America Lg Earthquake Mg Lg Rg P Li Velocity anomalies pP Q Attenuation			15. NUMBER OF PAGES 76	
			16. PRICE CODE	
17. SECURITY CLASSIFICATION OF REPORT Unclassified	18. SECURITY CLASSIFICATION OF THIS PAGE Unclassified	19. SECURITY CLASSIFICATION OF ABSTRACT Unclassified	20. LIMITATION OF ABSTRACT SAR	

## TABLE OF CONTENTS

Foreword	.....1
Phase Lg of earthquakes originated in southernmost South America and in Brazil	.....2
Mb <sub>Lg</sub> in South America	.....3
Rg in earthquakes originated in Peru, recorded in LPB station	.....3
Li waves in LPB station	.....3
Attenuation of seismic waves along paths Peru-Bolivia	.....3
Intensity attenuation beneath the central Andes in Bolivia	.....4
P-waves in South America	.....6
Analysis of seismic waves of short period in South America	.....9

## ANNEXES

- Annex 1 Magnitud mb<sub>Lg</sub> para sismos sudamericanos (R. Ayala)
- Annex 2 Atenuación de las intensidades sísmicas en la Cordillera de los Andes Centrales, Bolivia (R. Ayala)
- Annex 3 Anomalías de velocidad de las ondas elásticas en la región de Sudamérica ( J. Loa's thesis)
- Annex 4 Las ondas P en Sudamérica (M. Gonzalez's thesis)

DTIC QUALITY INSPECTED 1

Accession For	
NTIS	<input checked="" type="checkbox"/>
DTIC TAB	<input type="checkbox"/>
Unannounced	<input type="checkbox"/>
Justification	
By	
Distribution/	
Availability Codes	
Dist	Avail and/or Special
A-1	

## FIGURES

Fig. 1	Model of Brazilian structure	.....2
Fig. 2	Preliminary Q model for Peru-Bolivia	.....4
Fig. 3	Attenuation curves of intensities for different seismogenic zones in Bolivia	.....5
Fig. 4	Western South America showing the LPB station and curve representing the number of earthquakes	.....10
Fig. 5	Seismic zonation of South America	.....12
Fig. 6	Residuals related to the azimuth for LPB station	.....14
Fig. 7	Epicenters and residuals of Zone IX	.....15
Fig. 8	Time vs. distance for continental and oceanic earthquakes	.....17
Fig. 9	Sample of particle motion	.....17
Fig. 10	Spectra for Zones VII B and IX	.....19
Fig. 11	Type of signal for different zones	.....24
Fig. 12	Presence of P-derived phases	.....25
Fig. 13	Main features of plates	.....27
Fig. 14	Geotectonic units	.....27
Fig. 15	Tectonic map of South America	.....28
Fig. 16	Nazca Plate tridimensional	.....28

## TABLES

Table 1	Grouping of regions	.....11
Table 2	Residual anomalies	.....13
Table 3	Velocity at maximum penetration	.....16
Table 4	Phases according to particle motion	.....18
Table 5	Spectral values	.....19
Table 6	Type of envelope of P-coda	.....22
Table 7	Phases in P-coda	.....23

## FOREWORD

The study of regional phases is a far too ambitious program if all or most of regional phases should be analysed for the whole South America.

Facing that problem, two approaches are possible:

- To make a preliminary study for the whole region.
- To focus especial problems for a limited part of the region.

Both approaches were attempted in our case:

- General characteristics of Lg, Li and P-derived phases appearing on the P-coda, recorded in the La Paz Station (LPB) were considered for the whole South America (with some consideration of other stations for comparison purposes).

- Rg was studied more carefully for earthquakes originated in Peru.

- Attenuation for main regional phases was estimated for the path Peru-Bolivia. Intensity attenuation was estimated in seismogenic areas of Bolivia.

About this report we shall remark that subjects reported in 1990 and 1991 are being reported now very briefly.

## PHASE Lg OF EARTHQUAKES ORIGINATED IN SOUTHERNMOST SOUTH AMERICA AND IN BRAZIL

No seismicity is found in the eastern part of southernmost South America (southern Argentina and Atlantic coast south of  $49^{\circ}\text{S}$ ). The western part is active north of  $47^{\circ}\text{S}$ , but very little south of  $47^{\circ}\text{S}$ .

Those earthquakes are shallow, close to the contact of Antarctic and South American plates. Signals appear much attenuated in La Paz (LPB) records and very short. No Lg could be seen.

Brazilian shield, according to previous studies (Cabr , 1988 and 1989), has earthquakes with Lg recorded much larger than P-phase. Apparent velocity of Lg is  $3.55 \pm 0.05$  Km/s, being the corresponding period 0.5 to 1.3 s.

Apparent velocity of Rg is  $3.41 \pm 0.04$  Km/s; the period for the largest amplitudes is 1.1 s.

Li hardly could be seen, being its apparent velocity quite variable,  $3.8 \pm 0.2$ .

The largest ratio Lg/P is  $5.2 \pm 0.3$ ; but Rg is still larger, being  $\text{Lg/Rg} = 0.7 \pm 0.3$ ;  $\text{Lg/S}$  is  $5.2 \pm 0.2$ .

An earthquake occurred in exceptional location, off coast of southern Brazil, on February 13, 1990; no Lg is observed, but S is present very small.

The accepted model has a total crustal thickness of 35 Km (Oblitas, 1972). The P velocity model is showed in Fig. 1.

We may end this subject by stating that Lg is a good discriminant to distinguish quickly earthquakes originated in the Brazilian shield from those originated in southern part of South America.

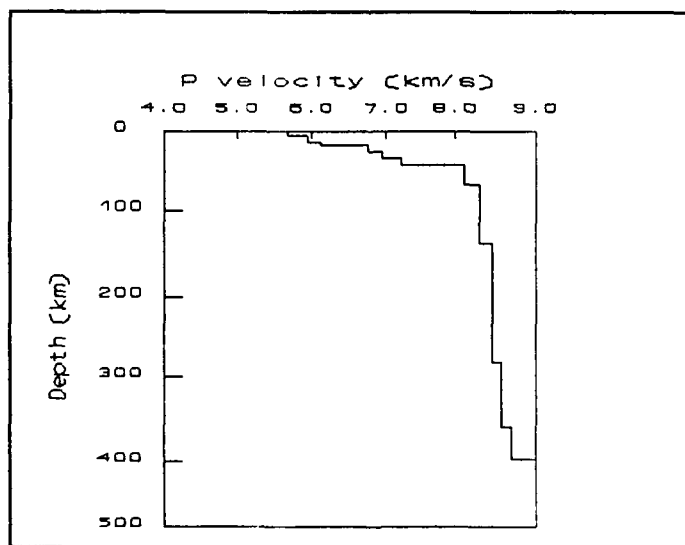


Fig. 1 Model of Brazilian structure.

## **mb<sub>Lg</sub> IN SOUTH AMERICA**

In several shield regions it has been found that Lg waves are a very good instrument for magnitude determination, since large wave amplitude allows a better precision than that of P-phase and the relation wave amplitude-magnitude is independent of the azimuth. In South America the problem is not so easy, since Lg amplitude depends strongly from the azimuth (changing the azimuth, we sweep very variable structures). Rodolfo Ayala succeeded finding acceptable equations for records at LPB Station, separately for cordilleran epicentral region:

$$mb_{Lg} = 3.80 + 2.00 (\log \Delta) + \log (A/T)$$

and for shield epicentral region:

$$mb_{Lg} = 4.40 + 1.15 (\log \Delta) + \log (A/T)$$

The paper presenting this study, as proposed for publication in Spanish (with an English abstract) is annexed to this report.

## **Rg IN EARTHQUAKES ORIGINATED IN PERU, RECORDED IN LPB STATION**

Rg waves, originated in shallow or intermediate depth earthquakes, travel through South America with a velocity between 2.8 and 3.4 Km/s; generally they have an emergent onset. Period lies between 0.8 and 1.5 s; wave amplitude depends mostly from the path focus-station:

- Very small from off coast of Peru.
- Fair from near coast of Peru.
- A little larger from continental north and central Peru.
- Largest from southern Peru.

Particle motion is characteristic of Rayleigh waves, probably resulting from the superposition of higher Rayleigh modes. Apparently Rg is transmitted along a channel, a granitic layer. The thesis of Celedonio Tito (in Spanish) was annexed to the scientific report No. 1 of September 1990.

## **Li WAVES IN LPB STATION**

This phase generally emerges in the earthquake coda and is masked by scattered waves, so that in very few cases its onset may be distinguished; any approximation of its velocity is very broad, but an interval between 3.79 and 3.96 Km/s seems acceptable.

Li is prevalent in horizontal components, transverse to the direction of propagation, that is to say, characteristic of shear waves, not visible at all for oceanic earthquakes originated farther than the boundary Nazca-South American plates.

The amplitude of predominant frequencies is highly relevant in the spectrum, what suggests a channeling layer, in the lower crust, very regular in the area.



## ATTENUATION OF SEISMIC WAVES ALONG PATHS PERU-BOLIVIA

Attenuation was considered for regional short period phases P, Li, Lg, Rg, originated in earthquakes both continental and oceanic of Peru, recorded at LPB Station.

Recorded amplitude (normalized for magnitude  $m_b = 5$ ) was plotted vs. distance for different homogeneous sets of earthquakes (same area and depth foci). The curves obtained were compared with a set of theoretical curves (Nuttli, 1973), corresponding to the equation:

$$A = K \cdot (1/\Delta^\circ)^{1/2} \cdot (1/(\sin(\Delta^\circ)))^{1/2} \cdot (e^{-\gamma \cdot \Delta^\circ})$$

The coefficient  $\gamma$  of anelastic attenuation corresponding to the best fit was accepted. After that coefficient and the group velocity (according to the formula:  $Q = \pi/T \cdot \gamma \cdot v$ ), the quality factor  $Q$  was obtained for focal areas. Finally  $Q$  was related to different depth and lateral structures (Fig. 2)

A paper (in Spanish) by Rodolfo Ayala is in press in the Revista Geofísica, Pan American Institute of Geography and History (PAIGH), Mexico. It was annexed in the scientific report No. 2 of October 23, 1991.

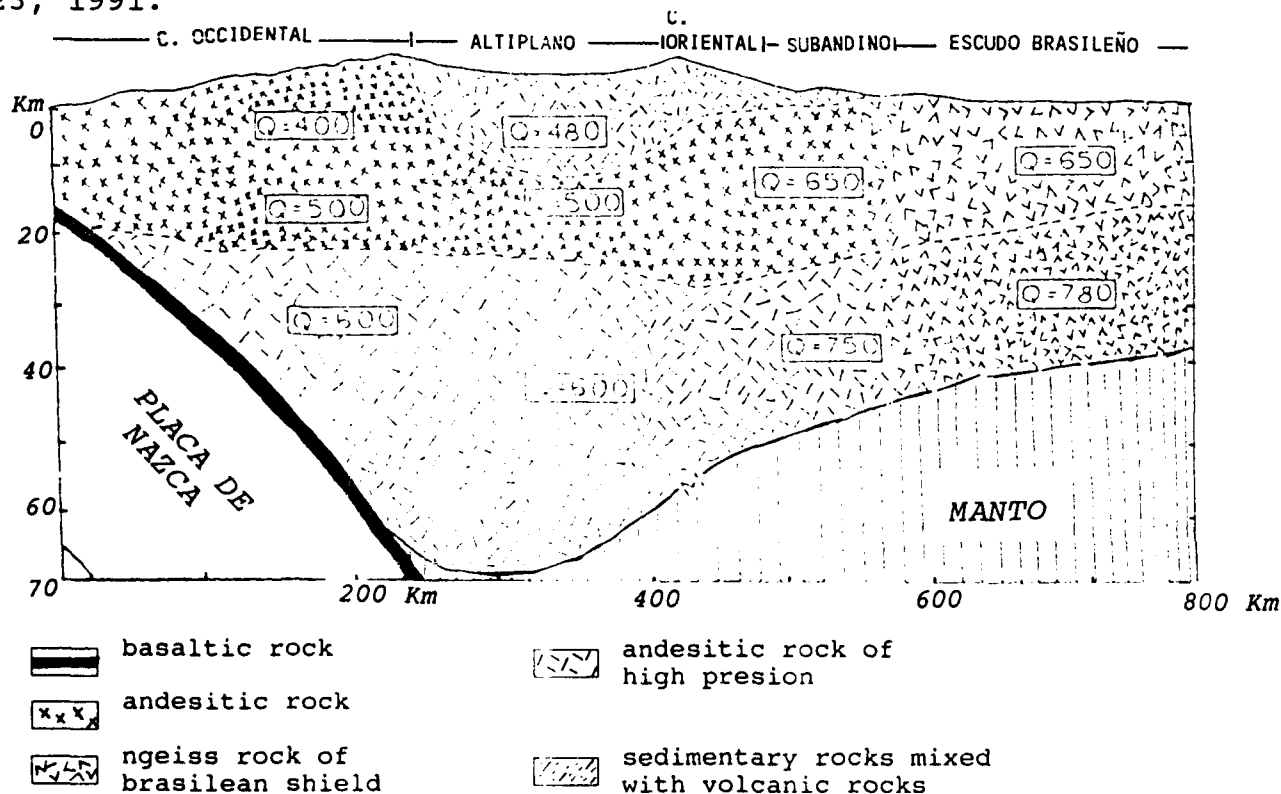


Fig. 2 Preliminar model of  $Q$  for the continental crust between Peru and Bolivia (crust model according to James, 1976).

## INTENSITY ATTENUATION BENEATH THE CENTRAL ANDES IN BOLIVIA

The generally accepted equation:

$$I(D) = I_0 + a + b \log D + cD$$

was the base for that study.

Bolivian felt earthquakes, from which sufficient information was available, were selected and grouped according to nine seismogenic areas.

Dealing with local earthquakes, it is necessary to consider that focal depth influences too much apparent attenuation; so focal (rather than epicentral) distances were used.

Starting from the values of intensity in each site and distance focus-site, coefficients  $a$ ,  $b$  and  $c$  of the above equation were found for the nine seismogenic areas. The corresponding attenuation curves are introduced through the fig. 6 in the paper of Rodolfo Ayala (in Spanish with English abstract) proposed for publication in the Revista Geofísica, PAIGH, Mexico, annexed to this report.

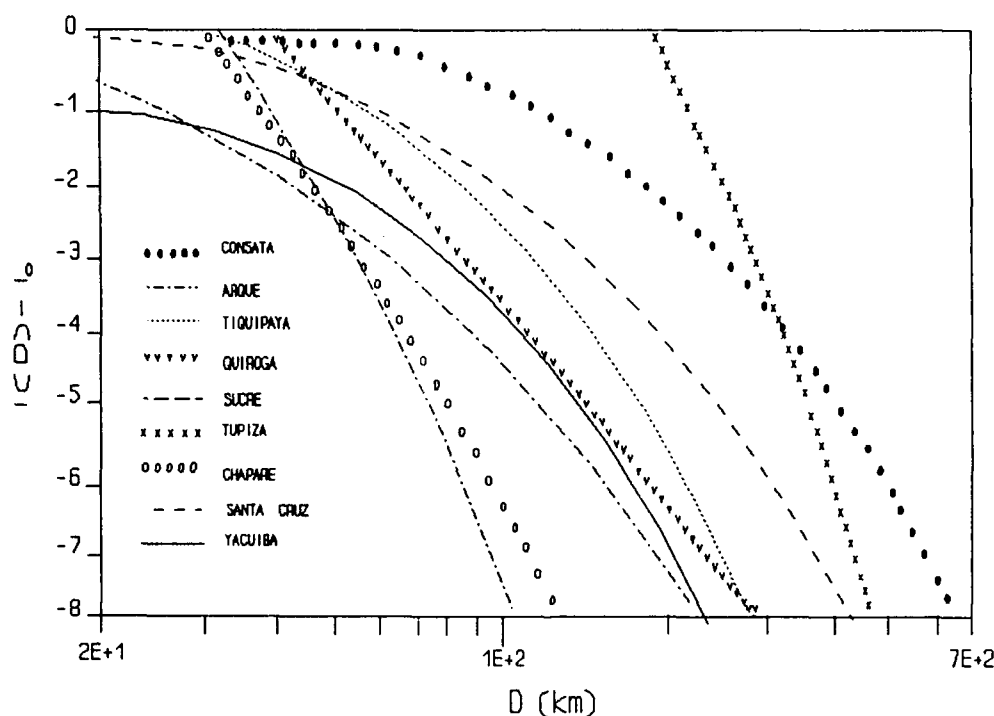


Fig. 3. Attenuation curves of intensities related with hypocentral distance for different seismogenic zones in Bolivia.

## **P-WAVES IN SOUTH AMERICA**

Abstract of Magaly González thesis: Las Ondas P en Sudamérica.

Longitudinal body waves P (also called compressional) produced in South America by the earthquakes of 1974-1989 (with some additions of especial interest of 1971-1974) recorded in the seismic station La Paz-Bolivia (LPB) are studied. The compiled events were originated at any depth until 643 Km, with magnitude 4.0 to 6.8, in the region, divided into 12 zones covering the whole continental South American plate and a part of Pacific oceanic plate; so we deal with both tectonically stable and unstable areas.

Basic foundations of seismology and some ideas of global plate tectonics, Nazca plate subduction and tectonic structure of South America are reviewed.

Particle motion, amplitude spectrum, absolute residuals, time-distance curves and P derived phases are considered fundamental processes for the research.

Particle motion has a direction parallel to the azimuth on the horizontal plane, smaller amplitude in the vertical plane perpendicular to the azimuth and maximum amplitude on the plane parallel to the azimuth, but a few exceptions may be found in some of the zones.

By means of Fourier transform amplitude spectrum is obtained, so determining the predominant frequency of P waves, their relation to the morphology of Nazca plate and realizing the structural complexity of the area.

Most of the absolute residuals related to the Herrin tables are positive; they change with focal depth, azimuth, distance and origin zone; this way anomalous zones of low velocity may be uncovered.

Time-distance curves allow to discover heterogeneities of the earth internal structure through which waves propagate; they also allow to quantify velocity at maximum of seismic ray penetration and some velocity changes related to distance.

Characteristics of waves, envelope types, wave amplitude and P derived phases appearing along a 30 s window were observed.

Statistical analysis of data and structure shows that transmission through continental crust for earthquakes located in the Caribbean curve is efficient for both shallow and intermediate earthquakes; on the contrary attenuation is large through the rest of the continent, especially for surface earthquakes.

The presence of lateral and vertical inhomogeneities in the crustal structure is confirmed through the study of spectra, residuals, particle motion and time-distance curves.

Delayed P arrivals to LPB for earthquakes originated in the oceanic plate correspond to a marked transition ocean-continent.

pP and Pn are relevant phases on the P-coda, compatible with E. Herrin's tables; other phases provisionally called P<sub>1</sub>, P<sub>2</sub>, P<sub>3</sub> and P<sub>4</sub> originate in discontinuities or interphases beneath South America at variable depth.

A large wave attenuation accuses a complex geological and tectonic structure.

Short period P waves allow an advancement of knowledge both of crustal structure and deep discontinuities.

#### VELOCITY ANOMALIES OF ELASTIC WAVES IN SOUTH AMERICAN REGION

Abstract of Jorge Loa Thesis: Anomalías de Velocidad de las Ondas Elásticas en la Región Sudamericana.

Seismic wave propagation contributes to the knowledge of internal Earth structure and its regionalization related to elasticity. Dynamical Earth processes are patent through the earthquake occurrence, their spatial-temporal distribution and mechanisms of energy liberation.

Any rock particle reacts as a forced but damped oscillator; it propagates movement received from previous particles, according to elasticity laws, being the propagation velocity of longitudinal waves:

$$v_p = [x + (\frac{3}{4})\mu/\rho]^{\frac{1}{2}}$$

and propagation velocity of shear waves:

$$v_s = [\mu/\rho]^{\frac{1}{2}}$$

The instantaneous state of vibration along a wave surface is represented by:

$$x = A \cdot \cos w(t - \tau)$$

Reflexion and refraction, according to the principle of Fermat and to the law of Snell, contribute to the distribution of energy. The curve time-distance represents a continued refraction, being its slope the inverse value of wave velocity at the maximum of seismic ray penetration, actually  $13.1 \pm 0.3$  Km/s was the maximum velocity noticed; it corresponds to intermediate depth earthquakes located in Zone IX.

P waves compress and dilatate the rock through which they propagate; environment may be solid or fluid; in it any particle oscillates in the direction of wave propagation. In local earthquakes crustal structure affects strongly surface motion; short waves are prevalent; if crust is typical of continent, a granitic layer gives rise to relevant waves of P nature.

Several wave trains, like pP, PP, etc., originate in processes of reflexion and refraction. The phase pP gives the best criterion to estimate focal depth; in the present study we have to remark that pP is not apparent in shield event records.

It has been customary to install short period (about one second) seismometers, three components and other three components for long waves (more than five seconds); early seismometers used purely a mechanical amplification; Galitzin introduced electromagnetic

amplification and seismographs of this kind were used in this study. Currently electronic amplifiers and magnetic recording are often used; on the other hand broad band seismographs are more and more in use.

In the present study 865 earthquakes originated in South America from 1975 to 1988 were used; they were recorded in short period seismographs installed in Seguencoma, La Paz; focal coordinates, origin time and magnitude were calculated by the International Seismological Centre.

Flinn-Engdahl regionalization was used as a base to sort geographically South American parts, but here another division is more appropriate.

Several different methods were employed; residual analysis, particle motion, spectral analysis and P-type phases in South America.

For the residual analysis recording time minus theoretical time (calculated according to E. Herrin's model) is considered; that difference is instrumental to know difference of existing structures, implying velocity anomalies in the earth interior related to the theoretical model.

Another method considers the envelope of seismic signals looking for different phases along the time record; that allows to hypothesize about structural changes, since the time record is a superposition of different seismic waves conditioned by their path. Together with that method, particle motion was used to determine wave nature, that is to say, to see if wave onsets correspond to longitudinal or shear waves, looking to the surface motion when seismic waves arrive; that motion is decomposed by means of three projections: on an horizontal plane, on vertical planes parallel and perpendicular to the azimuth.

Spectral analysis obtained after the Fourier transform (FFT method) was another tool; it converts the time domain into the frequency domain, obtaining an amplitude spectrum; the goal of this method is to distinguish prevalent wave frequencies for each epicentral area, to have relative amplitude and energy corresponding to each frequency of waves arriving to the station.

Through the study of P phases (pP, Pn...) in South America, recorded in La Paz, their best determination is sought.

The different methods give some results contributing to better knowledge of South America: the complex structure is a result of the interaction of four oceanic and one continental plates. For oceanic earthquakes the mean residual in La Paz is 2.6 s (2.2 s for shallow earthquakes, 2.7 s for intermediate focal depth); for those continental it is 2.5 s (3.6 s for shallow earthquakes, 2.2 s either for intermediate or for deep ones).

Among the P phases pP is a good indicator of focal depth, sP was observed in some earthquakes in the southern part of the region, sc. from 10°S to the south; other phases initially are called P<sub>1</sub>, P<sub>2</sub>, and P<sub>3</sub>.

## ANALYSIS OF SEISMIC WAVES OF SHORT PERIOD IN SOUTH AMERICA

### INTRODUCTION

Earthquakes in South America and western part of Nazca plate recorded in La Paz (Bolivia) LPB station have complex characteristics such anomalous residuals, several phases on the P-coda with abrupt changes of amplitude, making very different envelopes of the P-coda. These characteristics should be associated with different environments geological, tectonic, structural and seismic of South American continent.

Previous study (Cabr  S.J. et al., 1991) of earthquakes occurring in South America has shown the presence of the phases following the first P-arrival. Otsuka (1966) analyzed anomalous arrivals of P and pP. He used the array of the University of California at Berkely in the coast ranges; he found anomalies cyclic in the direction of the source, an azimuth anomaly of almost 10 degrees and a slowness anomaly of 1 s/degree.

Freedman (1966) studied possible errors in the observation in California and Nevada residuals of the Pn-phase from nuclear tests; she considered station corrections and found slow and unreliable travel times from the smaller explosions.

Rogers and his coauthors (1974) investigated the effects of topography on incident P waves.

Pennington (1984) investigated the effects of oceanic crust and subduction changes on phase .

Butler (1984) analyzed effects of azimuth, energy, attenuation and temperature relating them with amplitude changes of P waves.

Babuska (1984) calculated velocity variations of P waves in crystalline rocks.

Paulsen (1988) confirmed the existence of the discontinuity at 670 km depth, observing the conversion of P phases to S.

Kebeasy (1970) studied travel time anomalies in the north and east of Circum Pacific region.

Fiedler (1970) analyzed travel time anomalies of P waves across the crustal structure in the region of Caracas; he established a relation between residual and azimuth.

Sacks and his coauthors (1970) analyzed anomalies of P arrival times at an array of twenty seismographs in Chile, Peru and Bolivia and they concluded that residuals increase with station elevation. Data of aftershocks the Chilean earthquake of March 1985 and of some additional earthquakes of 1981 were studied to uncover tectonical details of Central Chile (Eissenberg et al., 1989).

Location by local seismographs was compared with that calculated from teleseismic data. It was concluded that location from local data is more accurate and consistent than that from remote stations.

The locations of small earthquakes recorded by local networks suggest that there are several fractures and flexures in the subducting lithosphere south of 33°S; but those fractures and

flexures are not noticed when only teleseismic stations are used for the locations.

Tectonical structures of South America and Pacific coast originate seismic velocity changes, which should not occur in areas of simple structure, or also originate a longer path through materials of lower velocity (sedimentary layer may be extraordinarily thick, lower velocity layers thicker than elsewhere have dipping boundaries, a higher temperature is maintained in some rock volumes).

Subducted Nazca Plate originates waves reflexions and refractions, with the result of new phases (different from the typical phases pP, sP, Pn...)

#### DATA

Seismic parameters were taken from the International Seismological Centre (ISC) Bulletins from 1975 to 1988 and, for several regions of low seismic activity, from those of 1971 to 1991. Almost 1500 events were analysed, although only 900 were useful. First, station LPB (La Paz, Bolivia) was considered; an initial comparison of the presence of phases after the first arrival from all the zones being studied was made using the seismic network of the Observatorio San Calixto; the regions 35-528 (Zone XXXV) and 9-143 to 146, (Zone IX) were analysed using also other stations of the World-Wide Standard Station Network (WWSSN) located in South America (Figs 4 and 5). The standard model of Herrin (1968) was used to calculate residuals. It uses a near-surface thickness of 40 km and P-wave velocities of 6 km/s to a depth of 15 km, 6.75 km/s between depths of 15 and 25 km and 8.049 km/s in the uppermost mantle.

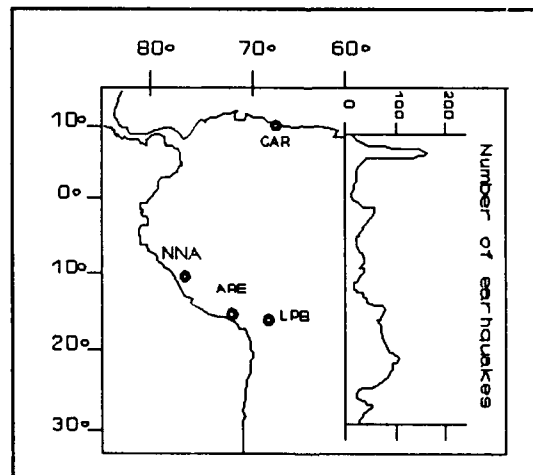


Fig. 4 Western South America showing four of the stations (●) used in this report. The curve representing the number of earthquakes per degree of latitude is on the right.

## METHODOLOGY

This study is based on analysis under the following headings:

- Grouping of seismic-geographic regions of South America
- Residual anomalies
- P-wave velocity at the maximum depth of penetration
- P-wave particle motion
- Spectral amplitudes
- Type-P phases in South America

### GROUPING OF SEISMIC-GEOGRAPHIC REGIONS OF SOUTH AMERICA

Four seismic zones (Table 1; Flinn and Engdahl, 1965) were considered, those numbered 7, 8, 9, 35; they cover most of the South American continent and parts of the Caribbean, Nazca and Antarctic plates bordering the continent.

Each seismic zone includes several geographic regions; the seismic zones take into consideration the degrees of seismicity in South America; regions 7, 9 and 35 are of comparatively low seismicity and of comparatively high stability; on the contrary, region 8 is of high seismicity; it is unstable and, in general, not in isostatic equilibrium. The South American region includes three principal geological environments: i) stable shield, ii) areas with a long history of slow geological evolution and iii) unstable zones, characterized by geosynclinal formation, active volcanism, mineral deposition, seismic activity and a complex relation of continental and oceanic structures.

Suggested the grouping of geographic regions into larger seismo-geographic zones (see Figure 5 and Table 1), which are parts of seismic zones of Flinn and Engdahl.

**Table 1**

Grouping of seismic-geographic regions into zones

ZONE	SEISMIC REGION	GEOGRAPHIC REGION	SEISMIC-GEOGRAPHIC NAME
VII A	7	97 98 101	Near coast of Venezuela E of 64°W Trinidad Venezuela E of 64°W
VII B		96 97 99 100 101	Near N coast of Colombia Near coast of Venezuela W 64°W Northern Colombia Lake Maracaibo Venezuela W of 64°W
VIII A	8	102 104 105 108 109	Near W coast of Colombia Off coast of Ecuador Near coast of Ecuador Off coast of Northern Peru Near coast of Northern Peru
VIII B		103 106 107 110 111 112 116	Colombia Colombia-Ecuador border region Ecuador Peru-Ecuador border region Northern Peru Peru-Brazil border region N of 10°S Peru N of 10°S
VIII C		113	Western Brazil



ZONE	SEISMIC REGION	GEOGRAPHIC REGION	SEISMIC-GEOGRAPHIC NAME
VIII D		114 115	Off coast of Peru Near coast of Peru
VIII E		112 116 117 118	Peru-Brazil border region S of 10°S Peru S of 10° Southern Peru Peru-Bolivia border region
VIII F		123 124 125 127 128 129	Northern Chile Chile-Bolivia border region Southern Bolivia Chile-Argentina border region N of 22°S Jujuy Province, Argentina Salta Province, Argentina
VIII G		121 122 134 135 136	Off coast of Northern Chile Near coast of Northern Chile Off coast of Central Chile Near coast of Central Chile Central Chile S of 37°S
VIII H		127 130 131 132 136 137 138 139 140 141	Chile-Argentina border region S of 22°S Catamarca Province, Argentina Tucumán Province, Argentina Santiago del Estero Province, Argentina Central Chile San Juan Province, Argentina La Rioja Province, Argentina Mendoza Province, Argentina San Luis Province, Argentina Cordoba Province, Argentina
IX	9	143 144 145 146	Off coast of Southern Chile Near coast of Southern Chile Southern Chile-Argentina border region Argentina
XXXV	35	528	Brazil

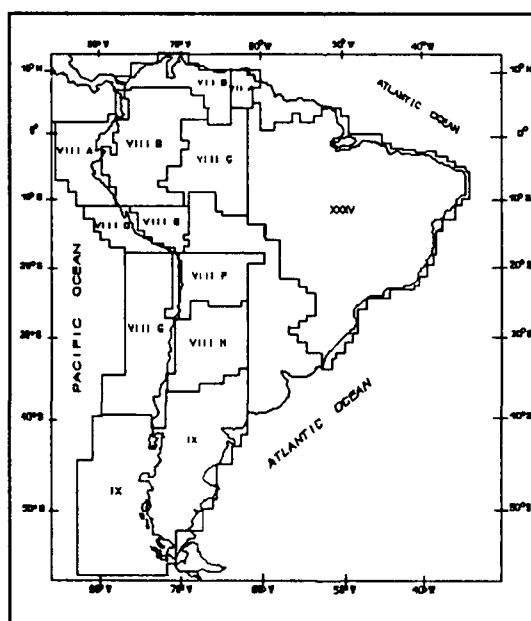


Fig. 5. Seismic zonation of South America used in this report (Roman numbers taken from Flinn and Engdahl, 1965; capital letters correspond to our subdivision).

## RESIDUAL ANOMALIES

Seismic P waves traversing a path within the earth do not take exactly the time calculated for that path in a standard earth. But residual differences appeared between different South American structures, what means velocity anomalies in the earth interior related to the theoretical model (Herrin, 1968). Residuals are caused by the focal and station regions, as well as by the wave path between them; they are a summation of the following:

- Epicentral and depth errors, depending on the number of stations used
- Depth error
- Structural differences between the model and the real focal volume
- Structural differences between the model and the real station underground
- Structural differences between the model and the real wave path
- Reading error: originated in the emergence of the signal (and possible transcription error).

If a large number of events are used, statistical error compensation diminishes the errors as a whole. Location errors are inversely related to the number of stations used; these are irregularly distributed, most of them N-S; on the contrary, error in longitude is larger since very few stations are located in the eastern South America and none in the oceans at those latitudes. Error originating in the different path structure has been reduced by grouping earthquakes according to similar tectonics and structures.

Depth errors are as large as  $\pm 25$  km for surface earthquakes (depth less than 71 km); they are less for earthquakes of intermediate depth (71-300 km) and for deep earthquakes (depth greater than 300 km) used; these errors depend on the number and distribution of stations used.; that error has been lowered by using the pP phase. This way errors were maintained as low as possible.

**Table 2**

Residual anomalies S:surface depth; I:intermediate depth; D:deep

ZONE	AZIMUTH	DIS.°	DEPTH			RESIDUAL		
			S	I	D	S	I	S
VII A	190-196	26-28	24	116		4.0 $\pm$ 1.0	3.1 $\pm$ 1.5	
VII B	160-196	23-29	27	202		1.5 $\pm$ 0.2	2.5 $\pm$ 1.2	
VIII A	120-158	12-25	20	155		1.6 $\pm$ 1.6	2.6 $\pm$ 1.6	
VIII B	128-172	8-24	38	198		3.1 $\pm$ 1.9	2.0 $\pm$ 1.4	
VIII C	155-222	7-14	33	98	643	3.4	0.8	1.8 $\pm$ 0.4
VIII D	68-125	5-12	6	126		3.9	3.3 $\pm$ 1.2	
VIII E	40-134	1-10	60	272		2.4 $\pm$ 1.3	3.2 $\pm$ 1.1	
VIII F	304-30	2-11	33	275	605	2.2 $\pm$ 1.8	2.6 $\pm$ 1.3	1.8 $\pm$ 0.2
VIII G	11-65	3-24	19	77		3.6 $\pm$ 1.5	3.4 $\pm$ 1.7	
VIII H	336-12	9-20	50	201	623	4.3 $\pm$ 1.6	3.3 $\pm$ 1.5	2.6 $\pm$ 1.0
IX O	8-23	24-37	16	62		2.3 $\pm$ 1.6		
IX C	6-10	21-35	33	146		2.4 $\pm$ 2.1	2.8 $\pm$ 1.8	
XXXV	208-249	18-33	33			4.1 $\pm$ 0.5		

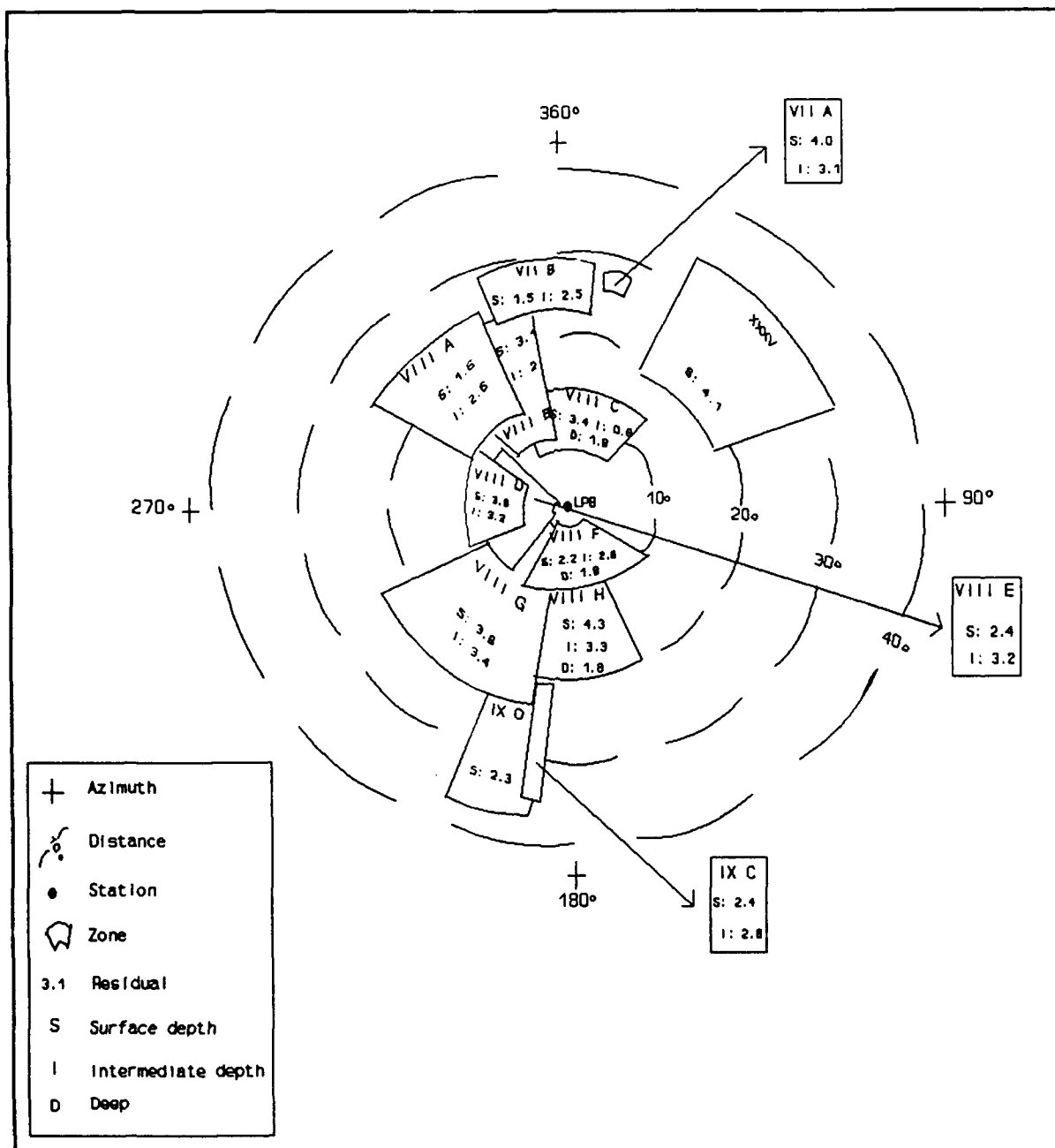


Fig. 6 Shows the position of mean residual in each zone related to the LPB station, that is to say, azimuth and distance to La Paz.

A residual means an anomaly related to the theoretical model, but that anomaly may be in the focus, in the path or close to the station, but probably in all three parts is different. Trying to

shed more light on the matter, we studied Zone IX in detail. Continental earthquakes were taken separately from the oceanic ones; plotting oceanic earthquakes showed high residual dispersion. A correlation with structures: Continental, with surface and intermediate seismicity; and oceanic, producing earthquakes in the initial bending of the Nazca plate to be subducted and in fractures and transform faults at the contact between Nazca and Antarctic plates, Fig 7a.

The delay in the focal volume in oceanic structures is evident (see Fig. 7b) because of its complexity compared to continental structure. A similar effect appears in the other WWSSN stations, where a path delay is found at transition ocean-continent, though delays change from one station to another.

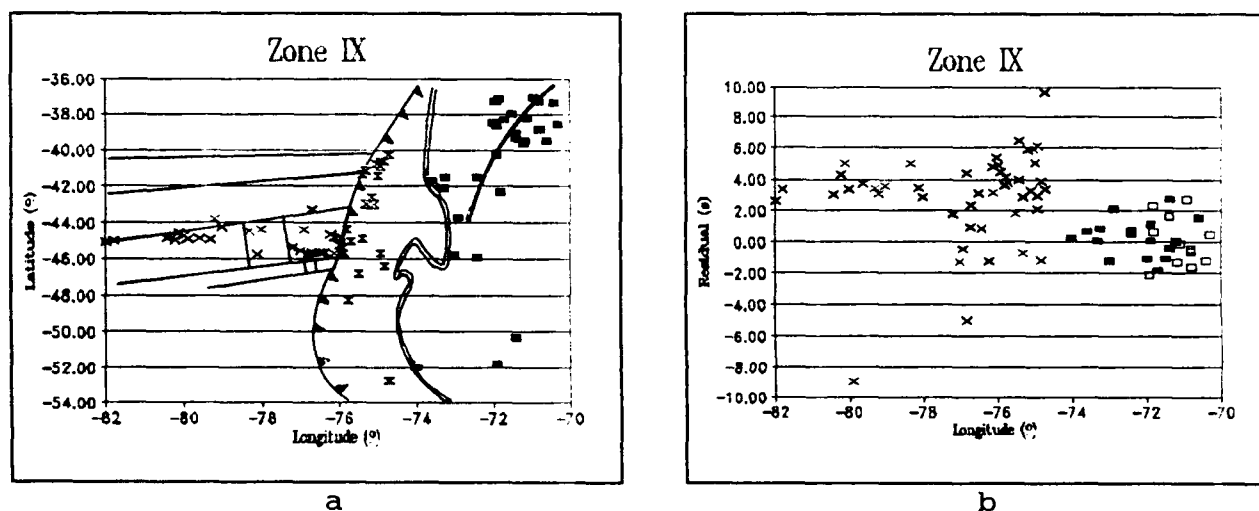


Fig. 7 a) Epicenters of Zone IX with indication of: volcanoes (—), coast (—), line of subduction (—), oceanic features (==), continental epicenters (■) and oceanic epicenters (x, x); b) Residuals vs longitude of epicenters: oceanic earthquakes (x), continental earthquakes (shallow depth ■ and intermediate depth □).

#### P-WAVE VELOCITY AT THE MAXIMUM DEPTH OF PENETRATION

The velocity changes in the interior of the earth, generally increasing with depth, become apparent by plotting time versus epicentral distance.

Other empirical curves time-distance show irregularities, which may originate in local errors (because, for example data were scarce or P waves arrived within the coda of another shock) or may correspond to anomalies such as those happening in the Bucaramanga nest at

7.17°N of latitude and 73.18°W longitude (junction point of Nazca, Caribbean and South American plates) the south end of subduction, of zones VII A and VII B.

The inverse of the slope of the time-distance curve is the P wave velocity in its maximum depth of penetration within the earth; curves were plotted separately for surface earthquakes, earthquakes of intermediate depth and deep earthquakes.

Empirical time-distance curves show corners corresponding to changes of velocity with distance, that are abrupt in time; these reveal different media or structures represented by approximately linear segments; when the change of velocity is not so sudden, the join of the segment is practically invisible).

Actually we find the maximum velocity for records in LPB of South American earthquakes to be  $13.1 \pm 0.01$  km/s at an epicentral distance of 4050 km; for the standard model of Herrin, this corresponds to a depth of 2295 km. For distances between 200, and 1100 km  $7.9 \pm 0.01$  km/s is the maximum velocity; (velocity does not decrease faster than radius) corresponds to a depth of 65 km, apparently the deepest limit of the crust; this velocity does not, of course, correspond to the Herrin model, which has a velocity of 8.04 km/s between depths of 25 and 40 km.

Table 3 shows the measured velocity for maximum ray penetration for different epicentral distances in each region.

**Table 3**

Velocities at maximum penetration: IX O: oceanic earthquakes. IX C: continental earthquakes.  
sup: surface depth; int: intermediate depth

ZONE	DEPTH	CRUST	DISTANCE	SLOWNESS	VELOCITY	E %
VII A	sup int	20	2000-2800	0.090 $\pm$ 0.002	11.1 $\pm$ 0.2	2.2
			1200-2050	0.114 $\pm$ 0.001	8.8 $\pm$ 0.1	0.8
			1950-2800	0.098 $\pm$ 0.002	10.1 $\pm$ 0.3	2.0
VIII B	sup int	40	150-2000	0.120 $\pm$ 0.002	8.3 $\pm$ 0.1	1.8
			2000-2600	0.098 $\pm$ 0.003	10.1 $\pm$ 0.3	3.0
			1000-2000	0.120 $\pm$ 0.001	8.6 $\pm$ 0.1	0.8
			2400-2600	0.087 $\pm$ 0.012	11.5 $\pm$ 1.6	13.7
VIII D	int		200-950	0.123 $\pm$ 0.001	8.1 $\pm$ 0.1	0.8
			950-1450	0.119 $\pm$ 0.008	8.4 $\pm$ 0.6	6.76
VIII E	sup int	65	200-1100	0.126 $\pm$ 0.002	7.9 $\pm$ 0.1	1.6
			100-1200	0.113 $\pm$ 0.001	8.8 $\pm$ 0.1	0.9
VIII F	sup int	60	300-1200	0.122 $\pm$ 0.002	8.1 $\pm$ 0.1	1.6
			200-1100	0.117 $\pm$ 0.001	8.5 $\pm$ 0.1	0.8
VIII G	sup int	15	900-1200	0.117 $\pm$ 0.014	8.5 $\pm$ 1.0	1.8
			300-1000	0.121 $\pm$ 0.002	8.3 $\pm$ 0.1	1.6
			1074-2600	0.115 $\pm$ 0.001	8.7 $\pm$ 0.1	0.9
VIII H	sup int	50	1000-2200	0.122 $\pm$ 0.001	8.2 $\pm$ 0.1	0.8
			1000-2300	0.116 $\pm$ 0.001	8.6 $\pm$ 0.1	0.8
IX O IX C	int sup int	35	2800-4055	0.762 $\pm$ 0.001	13.1 $\pm$ 0.01	0.1
			2400-4000	0.082 $\pm$ 0.002	12.2 $\pm$ 0.3	2.4
			2300-2900	0.082 $\pm$ 0.002	12.2 $\pm$ 0.3	2.4
XXXV	sup	30	2100-3800	0.087 $\pm$ 0.001	11.5 $\pm$ 0.1	1.1

The analysis for Zone IX is shown in Figs 8a and 8b. The earthquakes in the continent were divided into surface and intermediate, resulting an acceptable fit, but for oceanic earthquakes that fit is impossible.

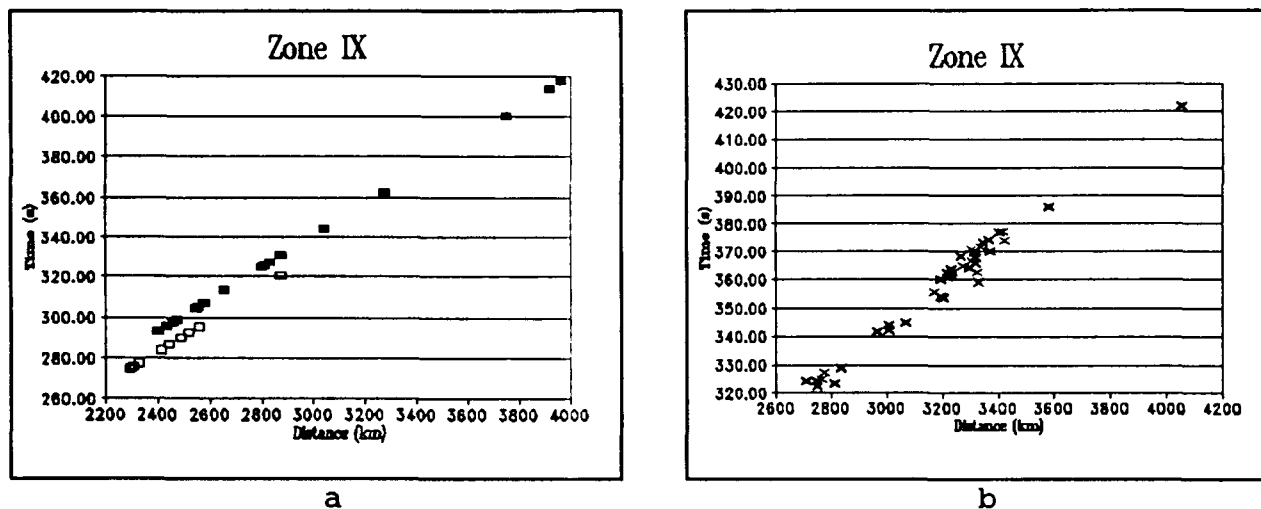


Fig. 8 Time vs Distance: a) for continental earthquakes (■ shallow, □ intermediate depth); b) x oceanic earthquakes

#### P-WAVE PARTICLE MOTION

Abrupt changes, both of amplitude and period appearing in the records of LPB station were analysed through the particle motion, we looked for different phases originating in refracting bodies or crustal anomalies and/or upper mantle anomalies.

Through the particle motion, P characteristics appear distinct in several cases, variable in others, or also rather complex. In Fig. 9 those characteristics mean: Motion is parallel to the azimuth in the projection on the horizontal plane, the vertical component being prevalent, but the projection on the plane perpendicular to the azimuth is small.

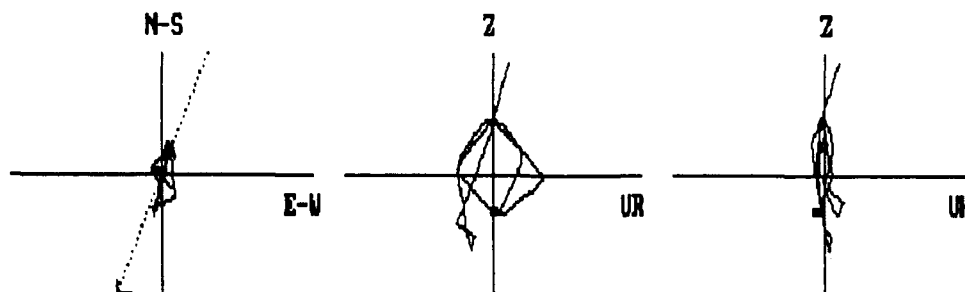


Fig. 9 Sample of particle motion; projections in planes of interest. 17

Sometimes P particle motion appears polarized in a plane not completely parallel to the vertical azimuthal plane. In some cases the horizontal projection of the particle motion is so small that almost it is reduced to a rectilinear segment; in those cases the projection on the vertical planes both parallel and perpendicular to the azimuth are very complex. From this analysis we conclude: there are three types of particle motion (typical, variable, complex) in P coda, changing according to the origin zone; duration of each phase was also established, together with the apparent velocity and record segments where interference prevents to show any well defined motion. Next Table 4 synthesizes that analysis.

**Table 4**  
Results of particle motion in each zone

ZONE	PHASE	TYPE OF MOTION	DURATION (s)	VELOCITY (Km/s)
VII A	P	variable	0.1- 2.5	9.0-8.9
	P <sub>1</sub>	variable	4.9- 9.4	8.9-8.8
	P <sub>2</sub>	variable	11.1-12.9	8.7-8.6
	pp <sub>2</sub>	variable	13.8-14.8	8.6-8.5
VII B	P	complex	0.1- 4.5	8.5-8.4
	P <sub>2</sub>	variable	11.8-12.7	8.2-8.1
	pp <sub>2</sub>	variable	19.1-20.0	8.0-7.9
VIII A	P	no obs.		
	P <sub>1</sub> P <sub>3</sub>	typical typical	2.5- 4.5 26.3-27.5	8.2-8.1 7.6-7.6
VIII B	P	variable	0.1- 1.6	8.5-8.5
	P <sub>1</sub>	typical	2.0- 5.7	8.5-8.4
	pp <sub>1</sub>	typical	16.7-18.2	8.1-8.0
	P <sub>3</sub>	variable	20.1-21.6	8.0-7.9
VIII C	P P <sub>1</sub>	no obs. complex	5.5- 7.5	7.5-7.6
VIII D	P P <sub>1</sub>	no obs. variable	2.2- 4.9	7.6-7.5
VIII E	P	typical	0.1- 2.3	7.5-7.3
	P <sub>1</sub>	variable	6.7- 7.6	6.9-6.8
VIII F	P	no obs.		
	P <sub>1</sub> P <sub>2</sub>	complex typical	1.5- 3.4 17.5-24.0	7.2-7.0 5.9-5.5
VIII G	P	typical	0.1- 2.5	8.3-8.2
	pp	typical	4.2- 6.3	8.2-8.1
	P <sub>2</sub>	typical	7.9- 9.3	8.1-8.0
	P <sub>3</sub>	typical	14.3-15.9	7.9-7.8
VIII H	P	variable	0.1- 0.3	7.9-7.8
	pp	typical	11.7-14.6	7.5-7.4
IX	P	variable	3.0- 4.5	8.5-8.4
	P <sub>2</sub>	variable	16.9-18.2	8.2-8.1
	P <sub>3</sub>	variable	26.0-27.7	8.0-7.9
XXXV	P	no obs.		

#### SPECTRAL AMPLITUDES

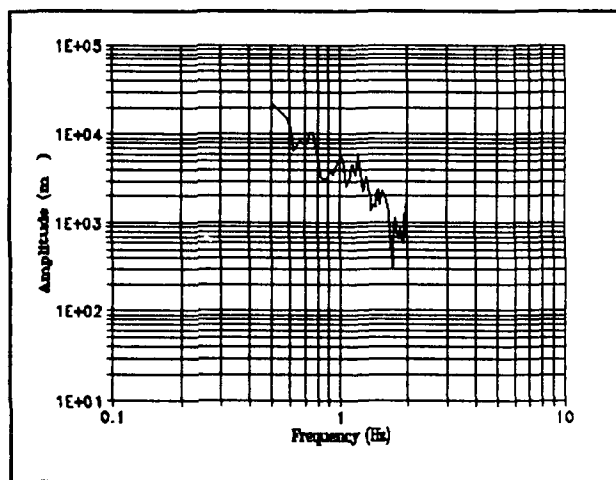
The magnitude corresponds to the energy radiated from the focus; to measure the energy arriving to the station, spectral analysis of the amplitude of motion contains relations to the wave path. In our

case wave path is across two large tectonic units covering the whole South American continent, one rather stable made up with shields (or cratonic zones), the other dynamically active identified with the Andean chain.

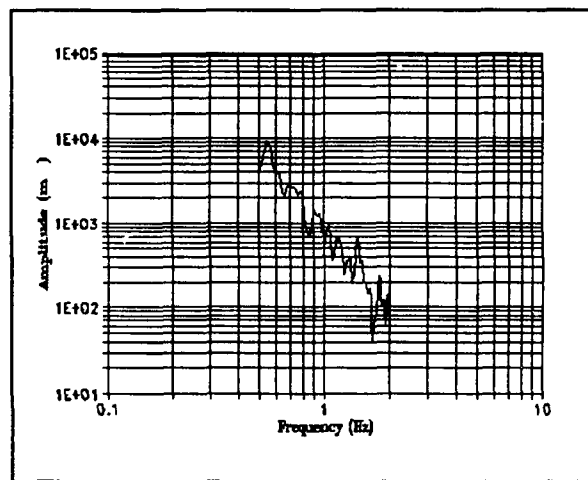
**Table 5**

Spectral analysis values.  $f$ =frequency (Hertz) corresponding to the largest peak;  $a$ =amplitude ( $m\mu$ )  $h$ = earthquakes depth (km);  $dist$ = epicentral distance of the earthquakes ( $^{\circ}$ );  $mb$ = earthquake body wave magnitude;  $Azi$ = azimuth

ZONE	DATE	$f$ Hz	$a$ $m\mu$	$h$ Km	Dist. ( $^{\circ}$ )	$mb$	$Azi$ ( $^{\circ}$ )
VII A	77-VIII-14	1.1	3405	112	27.9	4.2	192
VII B	78-VIII-08	1.21	6594	39	23.7	5	170
VIII A	81-IV-17	0.84	1870	33	21.9	4.2	145
VIII B	74-VIII-24	0.74	22144	91	22.5	5.7	158
VIII C	80-III-06	0.94	6067	67	10.7	4.8	164
VIII D	83-III-03	1.0	2945	63	10.5	5.6	119
VIII E	81-VI-05	0.89	7039	117	7.49	5.2	134
VIII F	74-VIII-04	0.7	23311	66	8.0	5.0	13
VIII G	75-I-01	0.8	16235	23	22.2	5.3	13
VIII H	75-IX-20	0.56	11170	50	16	4.9	2
IX	81-VII-28	0.55	28194	46	29.73	5	24
XXXV	76-III-22	0.99	1321	10	19	4.8	208



a



b

Fig. 10 a) Characteristic spectrum in Zone VII B; b) characteristic spectrum of Zone IX.

No clear relations between frequency of largest waves and local

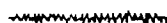


area appeared; the lowest frequency appears in earthquakes of the oceanic Zone IX, 0.55 Hz, the highest one in Zone VII B, 1.2 Hz (as we see in Figs 10 a and b)

#### TYPE-P PHASES IN SOUTH AMERICA

P waves in South American earthquakes recorded in LPB station were considered according to the initial character (emergent or impulsive) and the amplitude of wave train. According to their amplitude in LPB, earthquakes were distributed into three groups: small, medium and large.

-Records of small amplitude generally show an emergent beginning; a few exceptions are impulsive. (for example the earthquake in the figure has 4.8 mb and 18.96° epicentral distance)



-Medium size amplitudes may be clearly recorded after an impulsive beginning, or the contrary be emergent continued by interfering waves somewhat complex; in most cases abrupt changes are not observed, but generally gradual increases. (The earthquake below has 4.8 mb and 11.47° epicentral distance)



-Large waves frequently have impulsive beginning. (Earthquake in the example has 4.8 mb and 7.31° epicentral distance).



Let us see those characteristics by regions:

The zones VII A and VII B have small to regular amplitude waves, the onset is generally emergent.

The zones VIII A, VIII B and XXXV generally give small amplitude waves and emergent onset.

The Zone VIII B, in part of Ecuador and Peru-Brazil border, gives also small amplitude; but in the remaining part of the zone waves may be somewhat larger, to grow then gradually, generally the onset is emergent.

In the zones VIII D and VIII E for earthquakes near the Peru coast, waves initially are very small and increase gradually without reaching a fair amplitude; in the interior of Peru at the border of Peru-Bolivia waves have a smaller attenuation; the onset more often is emergent than impulsive.

In Zone VIII F the amplitude of the waves is regular to increase or grow gradually; this change is clear in the north of Chile about

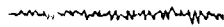
latitude 21°S. In the south of Bolivia and north Argentina the waves amplitude is much larger with emergent or impulsive onset. In zones VIII G and VIII H and IX we found regular and low amplitude waves; the onset is emergent and for a few seismograms impulsive.

Earthquakes with long duration (more than one hour) are localized in zones VII A, and VII B, VIII A, VIII B, VIII C, VIII D, and XXXV; in zones VIII E, VIII F, y IX the coda of the earthquakes in general is short.

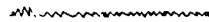
#### ENVELOPE TYPE OF SEISMOGRAMS

Statistical correlations between envelope type and magnitude, depth distance, source, path were attempted for each zone. We distinguish six types of envelope:

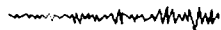
1 Amplitude almost constant



2 After a train of large waves, a decrease to continue uniformly with lower amplitude



3 A beginning of small waves then being enlarged gradually



4 A small wave train and then a step to large waves



5 Waves decreasing rapidly during a few seconds (no more than 10 seconds) with another wave train superposed:

5a first wave train smaller than the second



5b first wave train larger than the second



5c both wave trains equal size



6 Two or three short waves of large amplitude with interposed cycles of smaller amplitude



Envelopes are characteristic of each zone, so that only by looking the envelope figure you know the region of the earthquake (both focal volume and geology of the path determine that envelope). At the same time that analysis points out possible phases to be confirmed through the particle motion analysis.

Table 6 shows the correspondence of the envelopes to zones.

**Table 6**  
Type of envelope

ZONE	GEOGRAPHIC REGION	TYPE OF ENVELOPE
VI A	97	1
	98	1
	101	3-4
VI B	96	1
	97	1
	99	1
	101	3-4
VIII A	102	1
	104	1
	105	3
	108	1
	109	1-2
VIII B	10	1
	107	1-4
	110	1-4
	111	1-4
	112	1
	116	1-4-5a
VIII C	113	1-3
VIII D	114	1
	115	1-5a
VIII E	116	1-5a
	117	1-5a
	118	5a-6

ZONE	GEOGRAPHIC REGION	TYPE OF ENVELOPE
VIII F	123	4-5b-5c 6
	124	4-5a-5b 5c-6
	125	2-5a-5b-6
	127	2
	128	2
	129	4
VIII G	121	4-6
	122	1-4
	134	1-4
	135	1-4
	136	1-4-6
VIII H	127	1-5c-6
	130	4-6
	131	6
	132	6
	136	4
	137	4
	138	6
	139	1-2
	140	5a
	141	5a
IX	143	1-5a
	144	1-2
	145	1-5c
XXX	528	1

#### TYPE-P PHASES IN DIFFERENT REGIONS

Discontinuities or heterogeneities in the interior of the earth are responsible of several phases within the P-coda; the study of those phases sheds light on the earth's interior structure.

We review the 12 zones of South America (see Figs 11 and 12) for those P-derived phases. The most frequent phase is pP with an interval of time after P corresponding to focal depth; Pn, for distances shorter than 10°, is well known; sP is not infrequent. Other phases, provisionally called P<sub>1</sub>, P<sub>2</sub>, P<sub>3</sub> and, exceptionally, P<sub>4</sub> are originated in local structures. See Fig. 12 and Table 7.

**Table 7**  
Phases in P-coda

ZONE	GEO. REGION	P s	P1 s	P2 s	P3 s	pP s	sP s
VII A	98	P					
	97	P	4.0	12.8	26.8	12.0-26.8	
	101	P					
VII B	96	P		11.5			
	99	P	3.8	14.6	26.3	8.8-34.5	
	97	P					
	101	P	2.0				
VIII A	102	P	4.6				
	104	P	3.3				
	105	P	3.7		21.0	4.0	
	108	P	7.5				
	109	P					
VIII B	103	P		13.6	23.2	15.7	
	107	P		13.8			
	110	P	5.0		20.0		
	111	P	5.2	14.0			
	112	P		14.1	19.0		
	116	P		14.0			

ZONE	GEO. REGION	P s	P1 s	P2 s	P3 s	pP s	sP s
VIII C	113	P	5.6				
VIII D	114 115	Pn Pn	4.1	11.0	27.0	4.0-6.5	
VIII E	116 117 118	Pn P P		13.6 12.2	23.0	3.9 26.3	
VIII F	123 124 125 127 128 129	P P P P P P	2.4 4.7 4.8	17.8 17.3 17.4	25.8 23.6 25.7	3.8	31.3 31.4 34.8 33.0-45.0
VIII G	121 122 134 135 136	P P P P P	1.2 3.3 3.0	9.0 12.0		5.0 4.0-6.9 6.0	20.6 25.2
VIII H	127 130 131 132 136 137 138 139 140 141	P P P P P P P P P P	2.0 6.0 4.1 2.1	9.7 10.7 9.9 10.4	27.6	3.6-11.4 6.5-8.0 3.9-15.0 4.0-7.0 3.5-9.5	9.0-18.4
IX	143 144 145	P P P			23.0	7.0	19.5
XXXV	528	P					

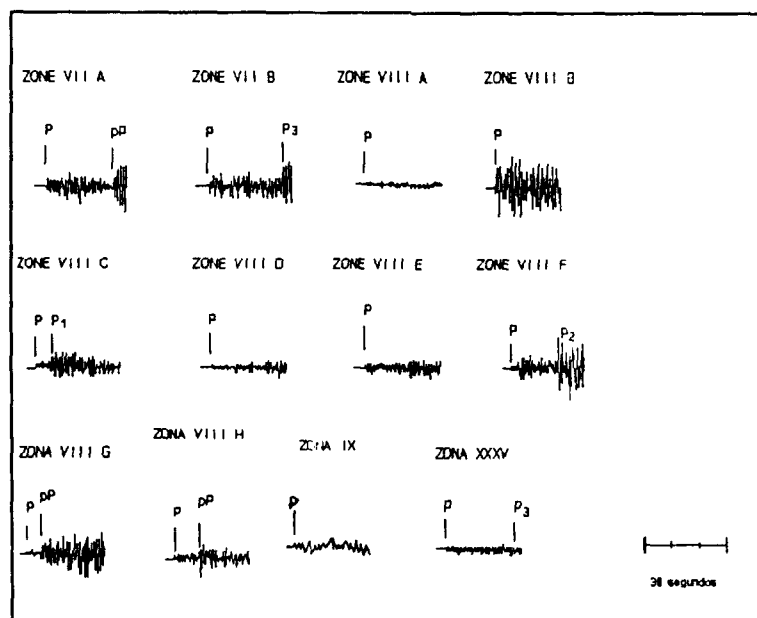


Fig. 11 Samples of type of signal according to different zones

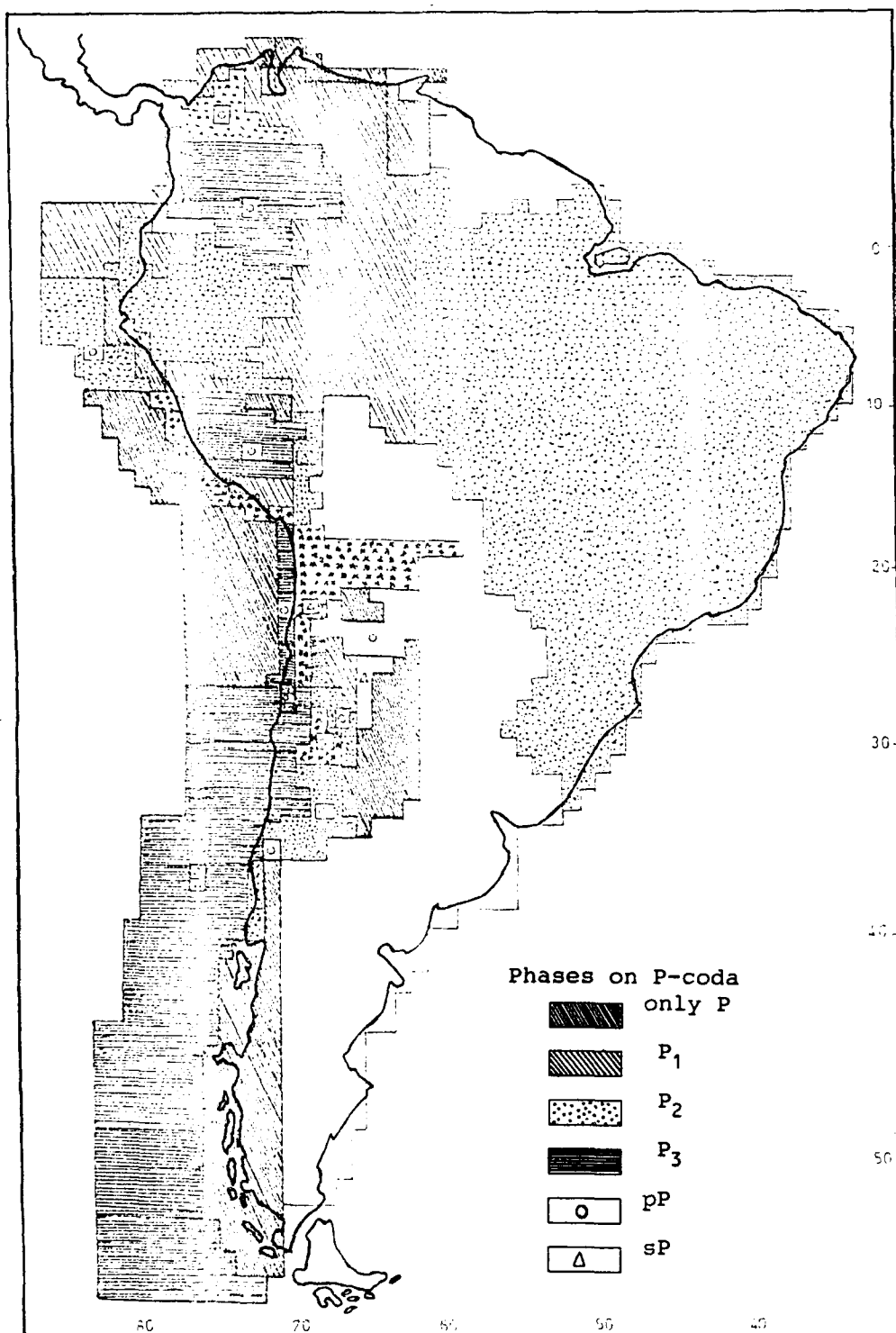


Fig.12 Presence of P-derived phases in LPB records according to origin zones

## ANALYSIS

### CARIBBEAN ZONES

In the Zone VII A, foci are grouped in planes perpendicular to the volcanic arc, where thrust faults are known, controlling the western Atlantic plate sinking by discrete blocks at the contact with the Caribbean plate, Fig.13.

In Zone VII B seismicity coincides with a part of the active tectonic belt bordering the Caribbean sea continued at the west end by the circum-Pacific orogenic belt (Fig.13).

At the western part of the Zone VII A, foci are shallow located in the Merida Cordillera along the Boconó fault (Bolt 1970); the zone to the east is compressed; oceanic origin and folded, recent formation is evident, the earthquakes being located in the Central Cordillera, Oriental Cordillera and Valles. In Santander province we find the Bucaramanga nest: it is a volume schematically of sides of 5 km and 170 km deep; that volume is stressed by the concurrence of Nazca, South America and Caribbean plates, so that it is an area highly weakened.

Geologically that zone is made up with posttectonic Andean basins filled with marine deposits and volcanic material; two geomorphic provinces are recognized: eastern planes of broad sabanas and the Andean region (Fig 14), the Merida Cordillera trending north-northwest and Sierra de Perijá as a continuation but trending north (Restrepo, 1970).

The predominant fault system in that zone (see Fig. 15) is parallel to the Andean Cordillera, most of faults are normal; the faults Oriente, Magdalena (constituted by Bucaramanga, Palestina, Boconó and Romeral faults) and Oca cross the zone east-west; the Romeral fault is relevant since it divides oceanic and continental crust; the system Boconó-San Sebastián-Pilar is the most active part; there is the largest relative movement between the Caribbean and South America so being the main limit between the two plates (Ropain and Alvarez, 1985).

Generally signals are emergent and small; time-distance plotting is disperse, so that maximum velocity remains undefined and it is impossible to estimate maximum ray penetration.

Residuals for epicenters near the coast are aleatory, meanwhile continental epicenters produce residuals homogeneous of one to two seconds.

Wave delay originates in two types of transition oceanic-continental, mantle-crust; but any way that delay is dependent on the distance.

For the Zone VII B the mean residual for surface earthquakes depends on the distance, still dependence on depth is more relevant.

Residuals of surface earthquakes without doubt are a focal effect; actually the area has an oceanic character of recent formation, but moreover it is a compression zone crossed by large faults, as that of Romeral; apparently the effects of path and station are minimal.

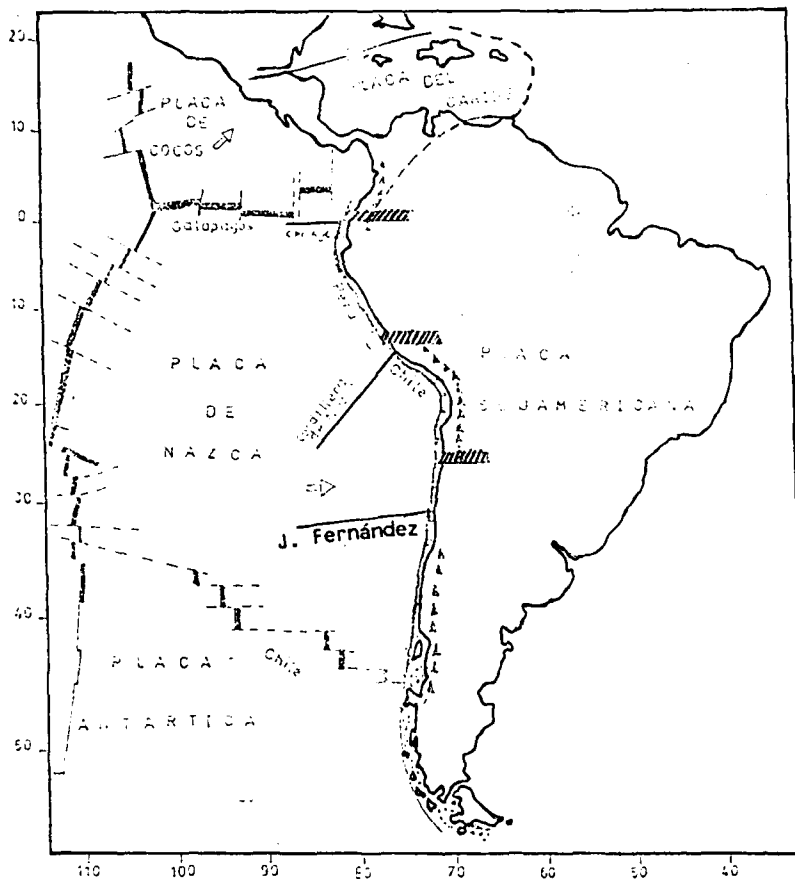


Fig.13 Main features of Caribbean, Cocos, Nazca, South American and Antarctic plates

- : Limit Between plates
- : Transition zones
- : Marine Cordillera
- : Subducted plate
- : Volcanoes

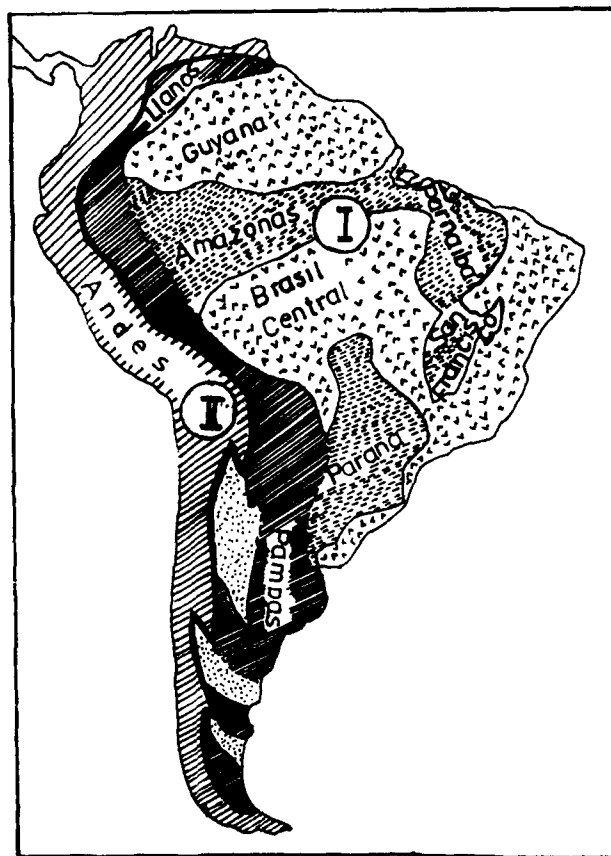


Fig.14 Geotectonic Units

- Shield
- Mesocraton
- Intracraton
- Pericraton
- Geosynclinal



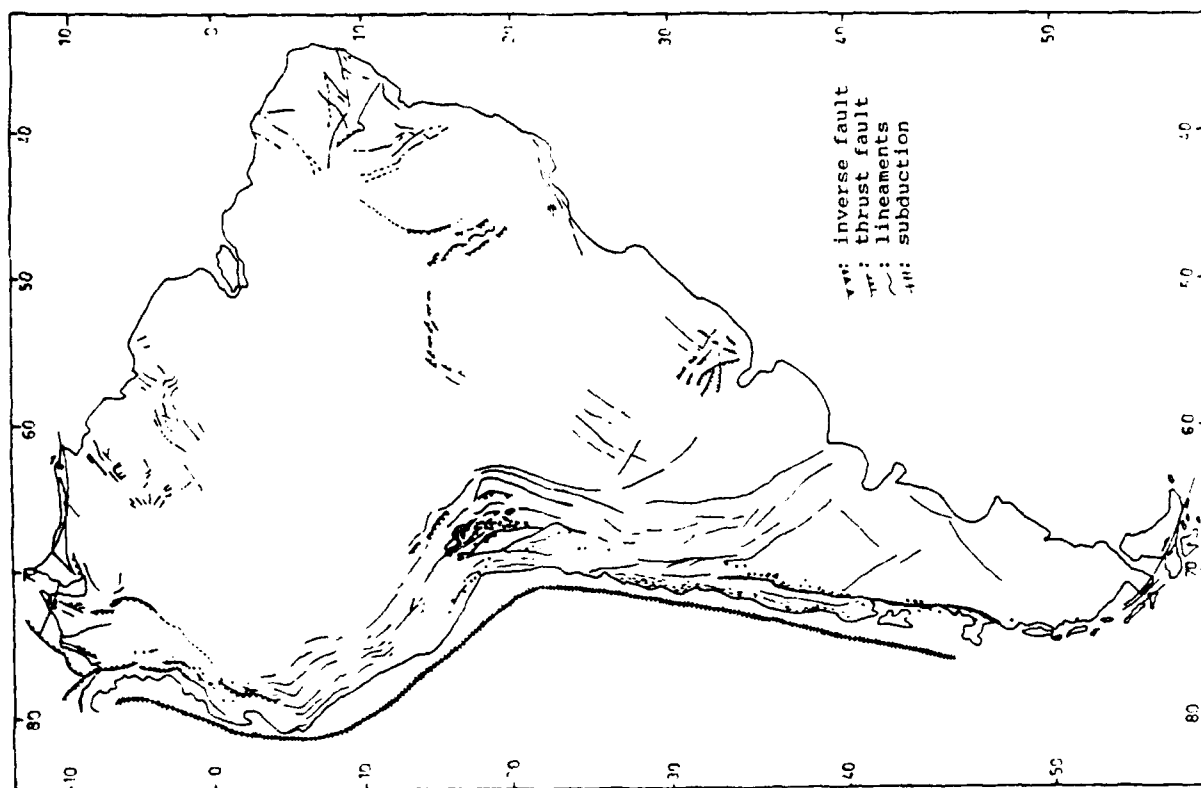


Fig. 15 Tectonic map of South America

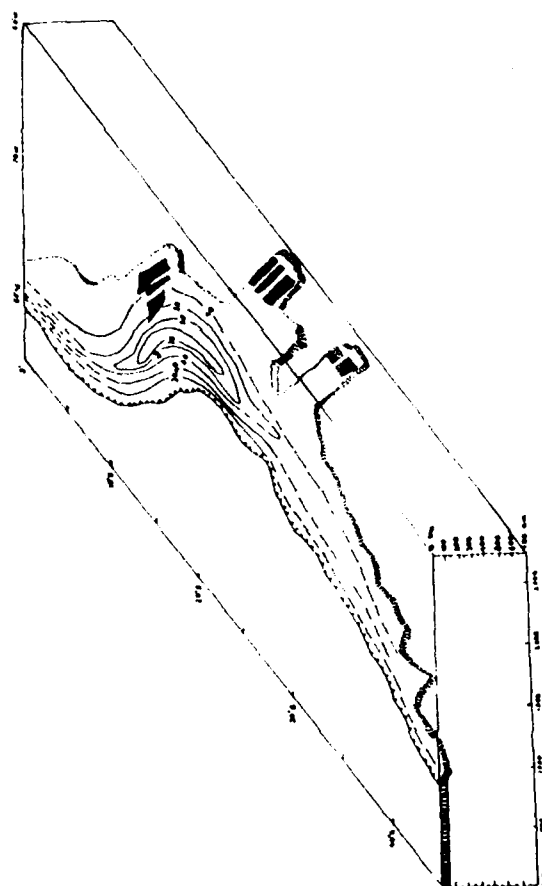


Fig 16. Nazca plate three-dimensional representation

When the focus is at intermediate depth, focus and station areas are more responsible for the residuals than the path, especially in the Bucaramanga nest where the zone is quite fractured.

Analyzing the P-coda of Zone VII A 4 phases were found, or amplitude changes for earthquakes located near the coast of Venezuela (mountain Zone of the Caribbean)

$P_1$  phase probably originates in the upper boundary of subducted plate, phases  $P_2$  and  $P_3$  were found only in surface earthquakes: probably  $P_2$  is a reflexion at the lower boundary of subducted plate and  $P_3$  through the transmission along the interface crust-mantle or it is originated in the low velocity layer at 200 km depth.

P Particle motion is variable.  $P_1$  and pP are present.

$P_1$ ,  $P_2$ ,  $P_3$  and pP may be present for earthquakes of northern Colombia (Zone VII B);  $P_2$  is found a few times for earthquakes of northern coast of Colombia and  $P_1$  appears also a few times for Central Colombia earthquakes

There are several possible hypotheses to explain those phases, being the most acceptable that considered above for the Zone VII A, considering the distance between that zone and the station LPB. P Particle motion is complex and changeable for the phases after P.

#### OCEANIC ZONES

The zones VIII A, VIII D and VIII G are characterized by seismicity in the oceanic crust and by the dipping of Nazca plate into the trench bordering Colombia, Ecuador, Peru, north and Central Chile, Fig 13. Epicenters of Zone VIII A concentrate close to the oceanic trench in the submarine Cordilleras Carnegie (see Fig.13), Grijalva and Sarmiento perpendicular to the coast. Here we find a seismotectonic transition zone established by Deza (1970) between  $0^\circ$  and  $1^\circ$ N (Fig. 13). The nature and location of seismic phenomena in the Zone VIII D suggests that there a large sliding takes place. The plate is subducted dipping  $10^\circ$  at the latitude  $12^\circ$ S, longitude  $79-77^\circ$ W (Fig. 16).

Tectonic and geological (see Figs. 14 and 15) background characterize the zone as a transition beginning at  $10^\circ$ S. The main morphostructural aspects are characteristic of Lima, Pisco and Arequipa basins, of the submarine Nazca Cordillera and fracture zone (Castillo and Huaco, 1963).

The fracture zone trends S-N subparallel to the coast line, being continental at 70 km from the coast, crossing to the ocean at the Paracas peninsula to coincide with the Lima basin (Huaco and Castillo, 1963).

At about  $13^\circ$ S there is a minimum of seismic activity characterizing a seismotectonic transition extending from  $10^\circ$ S to  $18^\circ$ S (Fig.13). The Nazca plate, in Zone VIII G, dips  $20^\circ$  towards the east at  $20^\circ$ S,  $70.6^\circ$ W, but decreases gradually so that it dips  $14^\circ$  at the latitude  $24^\circ$ S, only  $9^\circ$  at  $30^\circ$ S (see Fig.16). The mean thickness of Nazca subducted plate appears to be 105 km. Seismic surface activity is low (Minaya, 1978).

Juan Fernández islands and Challenger fracture cutting the trench

Peru-Chile near 33°S are important geological structures (together with Arica and Iquique basins), they are related with the volcanic gap extending from 28°S to 34°S (Mapa Tectónico de Sud América, 1978), Fig 13.

Signals are emergent with a few impulsive exceptions; the amplitude is small for the ocean earthquakes and fair near the coast, the Zone VIII G produces earthquakes both of short and long duration.

Residuals are dependent on the azimuth, distance and depth for the earthquakes located in the ocean.

The Zone VII A has smaller residuals for surface focus than for intermediate earthquakes. The delay for surface quakes is affected mostly by the focus and the station. The events near the west coast of Colombia have a smaller delay than those off coast of Ecuador, being the transmission in the first case through the shield, in the second case beneath the Cordillera and through the transition ocean-continent.

Intermediate depth foci occur at the beginning of the subduction, in this case wave delay is caused apparently by the transition ocean-continent and for near earthquakes by the transition crust-mantle beneath the station.

The Zones D and G have residuals a little larger for surface earthquakes, in contrast with the Zone VIII A.

In the Zone VIII D most distant earthquakes show residuals smaller; the near earthquakes show larger residuals, being their path through heterogeneous environments and crossing the transition ocean-continent (apparently here the last effect is stronger than in Zone VIII A).

Intermediate depth earthquakes occurring between 30°S and 40°S, in the Zone VIII G, are delayed mostly in the focal volume.

Summary of the analysis of P-coda for epicenters located in the ocean (Fig.12):

Phase  $P_1$  is the most common both for epicenters off and near the coast. Particle motion is variable.

$P_2$  appear seldom in zones A, D and G

$pP$  in Zone VIII G always arrives before  $P_1$ .

$P_3$  for earthquakes located in zones VIII D and VIII G probably corresponds to S converted to P.

$P_1$  actually corresponds to two possible origins: reflexion in the upper limit of subducted Nazca plate for surface foci; transmission along the interior of Nazca Plate for intermediate foci.

#### CONTINENTAL ZONES

The only common characteristic of zones VIII B, C, E, F, H and IX is the origin of most earthquakes in the interaction of plates, resulting to the geological accommodation. In the Zone VIII B the subducted Nazca plate is subhorizontal (almost parallel to the horizontal continental plate); the dip of Benioff zone is very small, but it increases to the south so that at 10°S dip is 12°, reaching seismic activity the depth of 200 Km. Here seismotectonic

transition between 13°S and 14°S is important (see Figs. 13 and 16).

Geomorphologically that zone is a continuation of VIII A; it consists of two provinces: los Llanos, flat lands and the Andean region (Fig.14), consisting of three cordilleras (Oriental, Central and Occidental).

Fault system ( Hall and Sevilla, 1985), (Fig. 15):

- Normal faults striking N-S parallel to the Andean Cordillera

- Dextral faults striking NE-SW

- Sinistral faults striking NW-SE

Among the important faults we have to consider the Oriente fault, along the eastern side of Cordillera Oriental, dipping to the west. Pennington (1981) identifies that fault with the continuation until near the border Colombia-Ecuador of the contact between Caribbean and continental plates.

Romeral fault striking N-S extends since Ecuador more than 800 Km towards the north, dipping to the E, separating the Cordilleras Central and Occidental, also dividing oceanic crust to the west and continental to the east.

Another fault parallel to Romeral, belonging to its system, is called Cauca fault.

In Ecuador faults striking N-S are associated with the interandean valley long more than 300 Km and 30 Km broad; that valley divides a row of active volcanoes making up the Cordillera Occidental and another row of extinct volcanoes making up the Real Cordillera of Ecuadorian Andes; many lineaments, generally thrust faults NE-SW, are remarkable in this part.

The faults Pallatanga and Guayaquil, striking NW-SE extend since the Amazonic basin until Andean western side along 150 Km, are the most relevant.

Quilotoa, Nanaguilca, Guagua, Pichincha are volcanoes potentially dangerous in the Cordillera Occidental; Sangay, Tungurahua, Cotopaxi, Coyambe are dangerous in the Cordillera Real (Hall and Sevilla,1985).

The zone VIII C corresponds to the western Brazil (Fig. 14), it has an irregular low seismic activity: one superficial earthquake located about 62°W, 10.7°S; however the seismic activity appears until 650 Km (Fig 16).

Geologically a zone pericratonic and intracratonic (Fig. 14), consisting in the amazonic basin and a part of Guyana and Central Brazil shield occupy that part of South America (Mapa Tectónico de Sud América, 1978).

Nazca plate abruptly changes dip to 72° at 73°W with seismic activity until 650 Km depth, Minaya, 1978, (Fig. 16).

In the Zone VIII E plate movement originates anomalies characteristic of transition zones.

The deepest earthquake occurred happened at 270 Km depth; the Nazca plate is subducted changing the dip angle.

The geological environment in that zone is variable: the Cordillera de la Costa parallels the coast since Arica to Paracas (14°S) with

the Cordilleras Occidental, Central and Oriental they are the Andean system along the western South America striking SE-NW making an arc gently convex to west at 10°S (Huaco and Castillo, 1963). Along that mountain chain there are relevant physiographic and tectonic features, such as the Ancash-Satipo fracture alongated 600 km, originating many surface faults starting at 11°S, 73°W trending NW-SE; on the other hand the Andean Cordillera shows from the point of view of physiography an important characteristic at 13-14°S (Deza, 1970): the main

axis of the Cordillera changes its direction around 30° towards the east together with the coast line. The general system of faulting (Fig. 15), striking NW-SE especially in the Cordillera Oriental at 12-14°S; the fault curving to E is evident, striking E-W. Gravity data points out a transition between 13°S and 14°S, being positive the anomalies at the north, negative at the south (Pisco, Ica, Nazca) amounting -60 mgal (Deza, 1970), what means a thin crust at the north, thick at the south, unless rock density should change dramatically.

In the Zone VIII F seismicity is high and uniform until 275 km depth, where an aseismic interval separates the deep activity between 528 and 603 Km at 19.22°S, 63-65°W. Plate dipping at 19°S, 69°W is 43°, but it increases towards the south until 46° at 22°S, 68°W; then it is maintained until close to 26°S; the mean plate thickness is 110 Km (see Fig.16).

The Cordillera de la Costa, Pampas centrales (or Central Valley) ascending through large tectonic steps to the east, the Cordillera Occidental, Altiplano, Cordillera Central and Cordillera Subandina, are the main topographic structural lines originated by tectonism (Vicente, 1970).

There are two reverse faults of low angle related to faulting system called Precordillera Oriental between 21°S and 25°S, (Fig.15), historically known to have moved (Vicente, 1970).

Volcanic centers extend along the Andean region associated to subduction processes of Nazca plate underneath the western margin of South American plate; that volcanism occurs along fractures parallel to the Andean axis and to a line of volcanic calderas (10 to 25 km in diameter, for instance Wheelwright, Galan, etc.) what originated broad deposits of lavas and rhyolitic ashes, especially at northern Chile, where a high concentration of epicenters is well known (González-Ferran and Lorca, 1985); at Jujuy and Salta the Puna is a volcanic area with high activity ( many volcanoes are close to the Chile-Bolivia border) (Fig. 13).

The Zone VIII H has a high seismicity in San Juan Province, moderate anywhere else in the zone. That activity may be superficial or intermediate, except in San Luis and Santiago del Estero Provinces where instead of intermediate activity they have deep activity, especially in Santiago del Estero where the deepest earthquakes happened at 623 km (Fig.16).

Dip of Nazca plate is 66° at 26°S, it decrease to 41° at 67°S, to 39° at 68°S; mean thickness of the plate is 105 km (Fig.16).

The Cordillera de la Costa, Principal, Frontal, Pre-cordillera, the Argentinian Pampa and southern part of the Puna are the most important lineaments and structures with high tectonic activity, see Fig. 15.

In the Chaco-Pampean region there are deposits of alluvium, loess, flood flats; two faults are known to have had historical movements, San Juan and Causete, corresponding to the faulting system of the Precordillera Oriental, striking N-S dipping towards the east both at the west of San Juan and extending to north more than  $25^{\circ}$ S.

The zones VIII B and VIII C give signals of low or fair amplitude, after an emergent onset, meanwhile the Zones VIII E, VIII F and VIII H give signals rather complex; the signals coming from the Zone E recorded at LPB are of two types:

- Surface earthquakes located north of  $15^{\circ}$ S have small amplitude.
- Intermediate earthquakes of depth have fair or large waves, predominating the large waves in the border Peru-Bolivia and impulsive onset.

The onset for Central Chile is emergent.

Records of Zone VIII F may have three types of envelope either for waves small or fair (Fig.11):

- the first type of envelope shows a gradual decreasing amplitude
- the second type, inversely, shows a gradual increasing amplitude
- the third type has an abrupt increasing step after two or three cycles small.

Generally the onset is emergent when first waves are small, but also in some cases, considered the second type, they show an emergent onset and a quick increasing of amplitude. The first type is characteristic of north of  $21^{\circ}$ S; the second type for the south of  $21^{\circ}$ S.

The Zone VIII B appears highly heterogeneous, since residuals are really large for distances between 1200 and 2400 km. The velocity at the maximum of ray penetration appears to be 11.5 km/s for distances between 2400 and 2600 km, but that measure is not dependable, since the possible error is 13.7%

Deep earthquakes have the smallest residuals in each Zone. Generally intermediate earthquakes should have small residuals than shallow ones in the same zone, but in the zones VIII E and F they are larger.

The delay causes change from one Zone to another; we shall analyse them separately:

In the Zone VIII E a thin crust for Central Peru and a thick crust for southern Peru, together with a transmission close to the axis of the Andes are the main responsible for the residuals of surface earthquakes.

In the Zone VIII F residuals for surface earthquakes originate mostly along the path, since waves cross volcanic zones, the main delayer for elastic waves. There are more intermediate than surface earthquakes; the geofractures and hot volume in the focal regions originate scattering and delay, the delay is enlarged still along the path.

In the Zone VIII H the path for surface earthquakes is along the Andes Cordillera, so that waves are subject to scattering and delay caused by lateral heterogeneities such as hot volume in the volcanic zone and geofractures across which hot material coming from the mantle, crosses.

For intermediate earthquakes the main reason of delay would be in the focal volume and probably in the dipping of Nazca plate.

Phases following the first arrival:  $P_1$  is present for all the continental zones, not often and certainly not clear in Zones VIII B and C, in contrast with the Zone VIII F and H it is recorded often and clearly.

Particle motion in general is quite complex, probably corresponding in some cases to S waves converted to P, especially in the Zone VIII H.

The phase  $P_2$  does not appear for Zone VIII C, but is frequent in the other zones especially in the Zone VIII H.

The phase  $P_3$  is not frequent in records of earthquakes located in zones VIII B and H but in the two other zones is frequent and fairly clear.

A phase called  $P_4$  appears only in earthquakes of the Zone VIII F; it arrives 32 seconds after the first arrival.

For earthquakes of zones VIII B, F and H in some cases we find the pP phase.

The particle motion for P is clear in the Zone VIII E; in the other zones it is variable or P not observed at all.

The interpretation of those phases is similar in the Zone VIII A, being similar the distance to the station and the geometry of plate subduction almost horizontal, say subparallel to the continental plate; surface quakes give the phase  $P_1$  through a reflexion in the upper discontinuity of subducted Nazca Plate; intermediate quakes give the apparently same phase through the low velocity layer within the mantle.

$P_2$  originates in the reflexion in the lower limit of the plate or through the transition across that limit.

$P_3$  is a late phase possibly originated in the transition crust-mantle.

It was realized that P derived phases are produced only in Cordilleran areas, especially north of  $10^\circ\text{S}$ .

The most acceptable hypothesis:

- $P_1$ , appearing only for surface earthquakes, is a phase transmitted through a crustal low velocity layer

- $P_2$  is transmitted along the mantle low velocity layer

#### OCEANIC-CONTINENTAL ZONE

The Zone IX consists of ocean and continental areas (see Fig.2), nonetheless the seismicity is similar in the whole zone; across that Zone from the north we have the continuation of Nazca plate subduction, its most southern part until  $46^\circ\text{S}$ , where the convergence of Nazca and South American plates is interrupted by the interposition of Antarctic plate (Fig 13).

Wave behavior changes from one part to the other as much as the crustal thickness (15 km in oceanic crust, 35 in continental crust).

Nazca plate dipping decreases to the south, being that plate almost horizontal at the south end (Fig.16).

Seismic activity at the subduction decreases to the south; it is very low after 46°S.

The Cordillera Patagónica, Cordillera de la Costa (ending at about 45°S), Patagonides and Cordillera Principal are important geological structures of the zone (Fig 14).

The Subandean deformed band changes to asymmetric foldings of simple geometry with a gentle dipping of juncture lines, locally refolded and locally deviated to the eastern Patagonic Andes.

Large structural divisions may be distinguished in that domain; moreover a geosynclinal structure is known here in what the trend NW-SE is very similar to Colombia, meanwhile the trend E-W (in Tierra del Fuego) is similar to Venezuela (Vicente, 1970).

Volcanism is present between 33°S and 44°S (Fig 13).

Signals arriving from that zone are small or fair, any way short; records corresponding to events originated off south coast of Chile have a first onset very small and increase quickly to decrease then smoothly; signals originated near the south coast of Chile have a rather constant amplitude, though a small enlargement may be distinguished somewhat similar to that

occurring for the events off south coast of Chile.

For earthquakes originated beneath the ocean the delay is caused exclusively by lateral heterogeneities, especially by the volcanic chains interposed to the path. First it was found that the intermediate depth earthquakes have a larger residual possibly originated in the heterogeneities at this depth, at the end of Nazca plate and beginning of Antarctic plate, together with an added delay in the transition ocean-continent.

Continental surface earthquakes, on the contrary, have residuals larger than intermediate earthquakes, located beneath the ocean. Those aspects were corrected considering a new model; what was found indicate that the residuals are anomalous only for earthquakes located off coast line. So indeed the physico-chemical aspects may have large influence by the contact Nazca-Antarctic plates.

pP, P<sub>2</sub> and P<sub>3</sub> were noticed within the P-coda for earthquakes located off northern coast of Chile, see Fig 11; near the south coast of Chile and at the border south Chile-Argentina only direct P may be distinguished either looking to records or to particle motion analysis.

P<sub>2</sub> and P<sub>3</sub>, when present, may originate in the mantle low velocity layer and at the interface crust-mantle.

#### SHIELD ZONE

The Zone XXXV covers the geographic-seismic region of Brazil. No deep seismic activity in that zone, but only superficial (Fig.14).



Mean crustal thickness is 35 km (Oblitas 1972).

It is made from the Brazil and Guyana shields, Fig.14, what were consolidated from four ancient blocks, through magmatic and tectonic processes during the early Paleozoic; later on sedimentary basins were formed such as those Amazonic, Chaco, Parana and Parnaiba. The western margin of the shield is masked by the Andean and Pre-andean geosynclines, what may be considered a transition zone between shields and the Andean region (Grupo de Trabajo, 1979).

The waves velocity at the maximum of ray penetration at distances between 2100 and 3800 km is  $11.8 \pm 0.1$  km/s.

The mean residual of that zone is  $4.1 \pm 0.5$  s, really large considering that residual should be expected to be small according to the geology of the Zone and short distance to the station. After that residual should be attributed to the station, but the analysis in the network of San Calixto Observatory suggested that an especial transition mantle-crust in the cordilleran area is the responsible of wave delay.

The onset of P is so small that it is not noticed through the analysis of particle motion.

#### **HYPOTHESIS:**

##### **P-WAVE TRANSMISSION ALONG CONTINENTAL PATH**

The likelihood that the Andean crust be vertically homogeneous was confirmed in much of the zones, since rocks constituting the Andean roots are of a similar composition to those appearing at the surface, plutonic or volcanic. But in some areas like the Altiplano and the Cordillera Oriental that vertical homogeneity does not exist, since a velocity change shows that beneath the Altiplano there are about 30 km of sedimentary rock and beneath the Cordillera Oriental there are 5 to 10 km of sedimentary rock. On the other hand P-velocity from the northern part of South America to La Paz is high compared with other parts of the continent.

Nevertheless in Peru some phases of P-coda were interpreted as transmitted along a low velocity layer within the crust; such possible low velocity layer never will appear through refraction, but on the other hand it should concentrate energy appearing in a delayed phase.

In western South America Nazca subducted plate plays a role opposite to that of a low velocity layer, that is to say, waves transmitted approximately N-S arrive obliquely to the subducted plate and may be reflected by either the upper or the lower contact surface; but moreover waves may be canalized along the plate (with higher velocity, according to its lower temperature).

The limit crust-mantle is another important discontinuity since it allows Pn transmission for earthquakes of focal depth no more than 40 km.

A mantle low velocity layer at 100 and 200 km beneath the surface

canalizes P-wave energy, so originating another delayed phase.

### **P-WAVE TRANSMISSION ALONG OCEANIC CRUST**

The oceanic crust is made up with basaltic material arising from the mantle and a small thickness of sediments coming from the continent and covering basalts. That influences really much the transmission of P-waves.

Transition ocean-continent originates a delay of P-waves; that delay is larger in southern part of South America than in its northern part. Oceanic crust is thicker beneath oceanic cordilleras and the rock has a low velocity.

The different structures of the path may explain time anomalies.

### **ORIGIN OF P-PHASES**

P-derived phases appear mostly in Andean earthquakes, not in shield earthquakes; they may be realized in Colombia and western Brazil (not in Central Brazil or in the coast of Atlantic ocean), being that a case meriting to be studied more carefully, especially concerning earthquake location.

Assuming that premise, we may establish that important discontinuities, (such as the mantle low velocity layer, subducted Nazca plate, the brittle mantle-crust interface and the crust low velocity layer) originate double or also triple P.

Let us revise the main characteristics of those environments giving rise to the P derived phases.

The mantle low velocity layer is at 200 km beneath the earth surface, where wave velocity decreases as a result of a lower rigidity of that zone compared to the neighboring materials, being the central part of that layer about 150 km deep and being the velocity 6% lower than just at the Moho discontinuity; that velocity decrease means that the rock here is less rigid than the neighboring materials, reaching again the normal velocity at 200 to 300 km depth.

Below the low velocity layer the rock is somewhat heterogeneous so that one could think that waves across it do not fulfill propagation laws: almost all seismic waves change direction, losing energy.

Nazca plate (quite uniform of high velocity) is composed with a thin layer gabbro converted into eclogite, laying on the thicker and lesser velocity layer.

An hypothesis is maintained that subduction originates mantle olivine oriented producing anisotropy and consequently delaying seismic waves.

The Moho discontinuity is at depth 10 km beneath the oceanic bottom, but it may be at 65 km beneath the continent; that discontinuity, according to recent studies, is not flat but rather brittle with irregular topography, chemical and physical composition and crystalline structure.

Low velocity surface layer, that is to say the sedimentary layer, has especial conditions in its composition, stratification, morphology, different epochs, various thermal conductivity, rock humidity, intrusions; all that originate reflexions and refractions, or canalization along a guide layer, etc. what often gives rise to later arrivals after the direct P.

#### **MOST ACCEPTABLE EXPLANATION OF FORMATION OF WAVE TRAINS CONSTITUTING P-WAVES**

Wave attenuation and scattering are highly related to P-derived phases formation; they depend mostly on the conditions of the wave path.

-Attenuation corresponds mostly to the rock heterogeneity since the focus to the station.

The first 10 or 15 km bellow the surface are very heterogeneous, not only from one place to another, but, at any location, mineralogical composition, density, porosity etc. are very variable.

-Local earthquakes generally produce larger waves than expected; scattering in the crust more heterogeneous than normal, with constructive interference, are responsible of that; another cause, in some cases, is the wave canalization in some crustal layers, generally thin.

Scattering with constructive interference appears through a gradational change of frequency, made visible through filtering. The subducted plate moreover may originate abrupt changes of velocity.

#### **CONCLUSION**

Flinn and Engdahl (1965) divide the earth surface into 729 geographical regions, each distinguished with a number and name. According to the frequency of earthquakes they group the geographical regions, resulting 53 seismic regions; from those with number 7, 8, 9, 35 cover South America and near parts of Pacific and Caribbean.

These regions do not correspond to the geological environments (stable shields, area with a long history of slow evolution, unstable areas); so seismic regions have been divided into zones, maintaining the number of Flinn and Engdahl region and adding a letter.

Residuals may be originated by:

- 1) Transition oceanic crust-continental crust (close to the focus or the station), such as zones VIII B and IX.
- 2) Transition mantle-crust, changing according to the angle between the seismic ray and the discontinuity (actually inclined bellow the LPB station).
- 3) Low velocity layer (about 100 to 200 deep). The deep earthquakes (localized in zones VIII C, VIII F, VIII H) have rather large residual, 1.8 s to 2.6 s (though smaller than shallow and

intermediate 1.4 s to 4.3 s and 2 s to 3.4 s respectively). Possibly the slope of asthenosphere-lithosphere boundary, changing the angle of the seismic ray against that boundary, originates a larger path within the low velocity layer (asthenosphere).

4) Thick sedimentary layer (possibly around 30 km in the northern Bolivian Altiplano). That should affect especially shallow earthquakes, as it is zone VIII D.

5) Wave attenuation so strong that the first P arrival should be lost and a second larger wave train should appear as the first phase, as Zone XXXV and Zone IX especially for oceanic earthquakes

6) An especial case of previous possibility: Seismic waves from Brazil surprisingly have larger residuals and lesser amplitudes than those coming from the other places deemed more absorptive with lower velocity. The hypothesis of a fragment of an ancient subduction (east of current subduction) could explain that difficulty: the direct seismic ray crossing the discontinuities added by that ancient fragment should be attenuated so that it should not be visible on records, leaving the first place to waves diffracted bordering the obstacle.

7) Higher temperature in rock lodging an active seismic nest. Specifically the intermediate depth earthquakes of Bucaramanga nest have residuals larger than shallow earthquakes; the apparent anomaly disappears if deformation energy of frequent seismics converted to heat would lower velocity. The San Juan (Argentina) nest gives also high residuals.

8) Higher temperature in volcanic focal area such as it may be that of contact between Caribbean and South American plates (for Zone VII A the mean residuals is 4 s).

Spectrum: The wave frequency corresponding to the maximum amplitude, changes from one zone to another; it may be related to the dipping of subducted plate.

Phases in P-code: The P-code (in a time window about 30 s) envelope is simple for deep earthquakes, with no phase superposed before the pP. For shallow and intermediate earthquakes complexity of P-coda arises from clear onsets of phases P<sub>1</sub>, P<sub>2</sub> and P<sub>3</sub> or changes in amplitude (increasing or decreasing) because of the canalization of energy or by the scattering.

1) Well known phases pP and sP are some times clearly recorded.

2) Other phases:

P<sub>1</sub>, apparently a reflexion at the upper boundary of subducted plate. This phase was found in all the zones studied, except in Zone XXXV

P<sub>2</sub>, possibly a reflexion at the lower boundary of subducted plate. This phase appears clearly in zones VII A, VII B, VIII F and VIII G; in zones VIII B, VIII D, and VIII E it may be confused with changes of amplitude originated in the energy canalized or scattering; in Zones VIII A, VIII C and XXXV does not appear at all.

P<sub>3</sub>, canalized along the upper mantle low velocity layer. P<sub>3</sub> is clear for earthquakes in zones VIII B, VIII F, VIII G and VIII H. In the other zones it is ambiguous.

## REFERENCES

- Aki A. (1973). Analysis of the seismic coda of local earthquakes as scattered waves, *J. Geophys. Res.* **78**, 1334-1346.
- Anzoleaga R. (1962). Algunas consideraciones de la corteza por debajo de los Andes, tesis, Universidad Mayor de San Andrés (La Paz, Bolivia).
- Bolt B., Filder G., Dewey J.W. (1970). Earthquakes and tectonics in western Venezuela, *International Upper Mantle Project*, **II**, 119-129.
- Barr G., Robson R. (1963). Seismic delays in the Eastern Caribbean, *Geophys. J. R. Astr. Soc.* **7**, 342-349.
- Cabré R. S.J., Minaya E., Ayala R., Capriles M. (1991). Lg and others regional phases in South America. Scientific Report **2**, Phillips Laboratory, Air Force System Command, Hanscom Air Force Base, Massachusetts.
- CERESIS (1985). Mapa Neotectónico Preliminar para América del Sur, Proyecto SISRA **11**.
- Comisión de la carta geológica del Mundo (1978). Mapa tectónico de América del Sur, UNESCO.
- Comisión de la carta geológica del Mundo. (1964). Mapa geológico de América del Sur, Consejo Nacional de Pesquisas, Brasil.
- Comte D., Ponce L. (1990). Morphology of the Benioff zone and crustal seismicity around Antofagasta, Northern Chile, *Trans. Am. Geophys. Un. (Eos)* **71**, 1462
- Deza E. (1970). Zonas de transición sismotectónica en Proyecto Internacional del Manto Superior **II**, 143-156.
- Eisenberg A., Comte D., Pardo M. (1989). The need for local arrays in mapping the lithosphere. *Observatory Seismology: A Centennial Symposium for the Berkeley Seismographic Stations* (J.J. Liteheiser, ed.). University of California Press, Berkeley, 187-193.
- Freedman H., W. (1966). A statistical discussion of Pn residuals from explosions, *Bull. Seism. Soc. Am.* **56**, 677-696.
- Flinn E., Engdahl E. (1965). A proposed basis for geographical and seismic regionalization, *Reviews of Geophysics* **3**, 123-149.

- González-Ferrán O., Lorca E. (1985). Mapa neotectónico preliminar para América del Sur, (Informe nacional de Chile), Mapa Neotectónico Preliminar para América del Sur: Programa para la mitigación de los efectos de los terremotos en la región Andina (Proyecto SISRA) **11**, 31-36.
- Grupo de trabajo (1979). Estructura geológica y geofísica de América del Sur, Seminario de Planeamiento sobre el Programa Geofísico Andino y Problemas Geológicos y Geofísicos Relacionados, (C. L. Drake, R. Cabré S.J., eds), 11-20.
- Hanus V., Vaner J. (1978). Morphology of the Andean and Wadati-Benioff zone, andesitic volcanic, and tectonic features of the Nazca plate, *Tectonophysics* **44**, 65-77.
- Hall M., L., Sevilla J. (1985). Mapa neotectónico preliminar para América del Sur (Informe nacional de Ecuador), Mapa Neotectónico Preliminar para América del Sur: Programa para la mitigación de los efectos de los terremotos en la región Andina (Proyecto SISRA) **11**, 37-41.
- Herraiz M., Espinoza A (1987). Coda waves, a review, *Pure Appl. Geophys.* **125**, 499-577.
- Herrin E. (1968). Seismological tables for P phases, *Bull. Seism. Soc. Am.* **58**, 1193-1236.
- Huaco D., Castilla J. (1963). Zonas de fractura y regionalización sísmica del Perú, ed. Instituto Geofísico del Perú.
- Isacks B. (1988). Uplift of the Central Andean plateau and bending of the Bolivian orocline, *J. Geophys. Res.* **93**, 3211-3231.
- James D. (1990). Structure of the continental lithosphere and subducting plate beneath east-central Peru, *Trans. Am. Geophys. Un. (Eos)* **71**, 1463.
- Jeffreys H, Shimshoni M. (1963). The times of pP, sS, sP and pS, *Geophys. J. R. Astr. Soc.* **8**, 324-337.
- Jordan T. (1981). Global tectonic regionalization for seismological data analysis, *Bull. Seism. Soc. Am.* **71**, 1131-1144.
- Kinoshita H. (1982). Peru Chile Trench and Nazca Plate, *Andes Science*, Preliminary report of the geophysical studies of the Central Andes, University of Tokyo, Japan.

- Leeds A., Knopoff L. (1972). Surface wave dispersion in the Andes, Upper Mantle Symposium II, 205-225.
- Michaelson S. (1986). Upper Mantle structure from teleseismic P wave arrivals in Washington and Northern Oregon, J. Geophys. Res. **91**, 2077-2094.
- Minaya E. (1972). Relaciones físico-químicas de la placa de Nazca y emplazamiento de yacimientos minerales, tesis, Universidad Mayor de San Andrés (La Paz, Bolivia).
- Morrison P. (1962). Resume of the geology of South America, ed. Institute of Earth Sciences, University of Toronto.
- Nor A., Ben-Avraham A. (1981). Volcanic gaps in the consumption of aseismic ridges in South America, Nazca Plate Crustal Formation and Andean Convergence: Geological Society of America Memoir **154**, 729-740, (Kulm L., D and four others eds).
- Oblitas J.L. (1972). Estructura del escudo Brasileiro a partir de la dispersión de ondas superficiales, tesis, Universidad de Chile (Santiago, Chile).
- Ocola L. C., Meyer R.P. (1971). Crustal low-velocity zones under the Peru-Bolivia altiplano, Geophys. J. R. astr. Soc. **30**, 199-209.
- Otsuka M. (1966). Azimuth and slowness anomalies of seismic waves measured on the central California seismographs array part I: Observatorios, Bull. Seism. Soc. Am. **56**, 223-239.
- Ramírez E. (1968). Los volcanes de Colombia, ed. Academia Colombiana de Ciencias Exactas Físicas y Naturales **XIII**, 227-235.
- Ramírez E. (1947). Mapa sísmico y tectónico de Colombia, ed. Instituto Geofísico de los Andes Colombianos Serie A **13**.
- Restrepo H. A. (1972). Explicación del corte geológico por latitud 6° norte en la república de Colombia, Upper Mantle Symposium II, 419-428.
- Rogers A. M., Katz L. J., Bennett T.J. (1974). Topographic effects on ground motion for incident P waves: a model study, Bull. Seism. Soc. Am. **64**, 437-456.
- Ropaín C., Alvarez R. (1985). Mapa neotectónico preliminar para América del Sur (Informa Nacional de Colombia), Mapa Neotectónico Preliminar para América del Sur: Programa

- para la mitigación de los efectos de los terremotos en la región Andina (Proyecto SISRA), 11, 25-29.
- Sacks S., Saá G., Aparicio F. (1972). P travel time anomalies and structural implications in West Central South America, Upper Mantle Symposium II, 255-264.
- Schneider J. (1990). Is there asthenosphere beneath the continental lithosphere in east-central Peru, Trans. Am. Geophys. Un. (Eos) 71, 1449.
- Schinn D., Isacks B, Barazangi M. (1980). High-frequency seismic wave propagation in western South America along the continental margin in the Nazca plate and across the Altiplano, J. Geophys. Res. 85, 209-244.
- Silgado E. (1968). Historia de los sismos más notables ocurridos en el Perú (1515-1960), ed. Instituto Panamericano de Historia y Geografía IV, 193-241, México.
- Suárez G., Molnar P. (1983). Seismicity, fault plane solutions, depth of faulting, and active tectonics of the Andes of Peru, Ecuador, and southern Colombia, J. Geophys. Res. 88, 10403-10428.
- Tarling D. H. (1982). The crust of the earth, The Cambridge Encyclopedia of the Earth Sciences (D.G. Smith, ed.). Cambridge University Press, 164-188.
- Tellería J. (1970). Dinamismo sísmico bajo los Andes Centrales y Tectónica Global, tesis, Universidad Mayor de San Andrés (La Paz, Bolivia).
- Valencio D. (1981). Significado geodinámico y geológico de los datos paleomagnéticos de rocas Jurásico-Cretácico de América del Sur, Comité Sudamericano del Jurásico y Cretácico: Cuencas Sedimentarias del Jurásico y Cretácico de América del Sur 2, 701-714.
- Vicente J. (1970). Tectónica, Proyecto Internacional del Manto Superior I, 162-180.
- Vila F. (1970). Geología y geofísica marinas, Proyecto Internacional del Manto Superior I, 189-203.
- Zeuner F. (1956). Geocronología: la Datación del Pasado, Ediciones Omega S.A., Barcelona.



**ANNEX 1**

# MAGNITUD $mb_{Lg}$ PARA SISMOS SUDAMERICANOS

R. RODOLFO AYALA SÁNCHEZ \*

## RESUMEN

Se analizaron las ondas  $Lg$  provenientes de sismos sudamericanos, registradas en la estación sismológica de La Paz-Bolivia (LPB), para determinar las relaciones de magnitudes  $mb_{Lg}$  para las regiones de Cordillera y de Escudo, considerando el azimut, profundidad y distancia epicentral. Las relaciones generales  $mb_{Lg}$  obtenidas son:

$$\text{CORDILLERA} \quad mb_{Lg} = 3.80 + 2.00 (\log \Delta) + \log (A/T) \quad \Delta < 18^\circ$$

$$\text{ESCUDO} \quad mb_{Lg} = 4.40 + 1.15 (\log \Delta) + \log (A/T) \quad 10^\circ < \Delta \leq 34^\circ$$

Donde  $A$  es la máxima amplitud de la fase  $Lg$  leída sobre una componente horizontal de corto período en micrones,  $T$  su correspondiente período en segundos y  $\Delta$  la distancia epicentral en grados. Las magnitudes  $mb_{Lg}$  son válidas y aproximadamente iguales a las  $mb$  para un rango  $4.0 \leq mb \leq 6.0$ . Los valores medios del coeficiente de atenuación son:  $\gamma = 0.20 \pm 0.03 \text{ grados}^{-1}$  para la Cordillera y  $\gamma = 0.09 \pm 0.04 \text{ grados}^{-1}$  para el Escudo. En general las ondas  $Lg$  tienen mayor amplitud que las ondas de cuerpo.

## ABSTRACT

$Lg$  waves from South American seisms recorded at La Paz-Bolivia (LPB) seismological station were analysed. Relations for magnitude  $mb_{Lg}$  for the Cordillera and Shield regions, considering the azimuth, depth and epicentral distance were established. The general relations for  $mb_{Lg}$  are:

$$\text{CORDILLERA} \quad mb_{Lg} = 3.80 + 2.00 (\log \Delta) + \log (A/T) \quad \Delta < 18^\circ$$

$$\text{SHIELD} \quad mb_{Lg} = 4.40 + 1.15 (\log \Delta) + \log (A/T) \quad 10^\circ < \Delta \leq 34^\circ$$

Where  $A$  is the maximum amplitude of  $Lg$  phase of any short period horizontal components in microns for corresponding period  $T$  in seconds and  $\Delta$  epicentral distance in degrees. The magnitudes  $mb_{Lg}$  are valid and approximately equal to  $mb$  for values  $4.0 \leq mb \leq 6.0$ . Medium values of anelastic attenuation coefficient  $\gamma$  are  $0.20 \pm 0.03 \text{ deg}^{-1}$  for the Cordillera and  $0.09 \pm 0.04 \text{ deg}^{-1}$  for Shield regions. Generally the  $Lg$  waves are larger than the body waves.

\* Observatorio San Calixto, La Paz, Bolivia.

## INTRODUCCION

En la práctica el cálculo de la magnitud no es tan preciso y por ello es conveniente encontrar diversos procedimientos que sean más seguros, para lo que se considerará la magnitud  $mb_{Lg}$  como una alternativa. Debido a que la fase Lg es usualmente la fase más grande observada para pequeños eventos, puede ser más apropiada para determinar la magnitud. Baker (1967 y 1970) determinó la magnitud (M) de un sismo a partir de la fase Lg (ver Tabla 1), postulando que los factores de atenuación de Lg pueden ser calculados por regresión lineal para cualquier rango de distancias. Los valores así calculados de M parecían dar mejores resultados para distancias epicentrales mayores a los 200 km que las medidas a partir de las fases directas P o S.

Sindorf (1972) a partir del estudio de la fase Lg de registros de sismos locales y sismos cercanos regionales, considerando sismogramas verticales de corto período para el Observatorio de Palmer (Estados Unidos), calcula la magnitud  $M_{LZ}$ , estando el período entre 0.2 y 2.0 s.

Nuttli (1973) calcula la magnitud de la fase Lg a partir de sismos de la parte este de Norte América; cita que las fórmulas empíricas calculadas para sismos del este de Norte América dadas por Evernden (1967), Nuttli (1969) y Evernden et al. (1971), para el cálculo de la magnitud de las ondas de cuerpo y superficiales, son del tipo:

$$M = B + C (\log \Delta) + \log (A/T) \quad (1)$$

Donde: M = Magnitud

B = Coeficiente que depende de la excitación en el foco o del movimiento de la onda de período T

C = Relación del coeficiente de atenuación de la onda con la distancia.

$\Delta$  = Distancia epicentral en grados

A = Amplitud máxima de la onda (de cuerpo o superficial)

T = Período en segundos

Las ondas Lg son ondas superficiales de corto período con niveles de excitación similares a los de la onda P de corto período y ondas superficiales de largo período, Nuttli (1973) sugiere que están más directamente relacionado a  $mb$  que  $Ms$ . También determina que la relación  $\log (A/T)$  versus  $\log \Delta$  es solamente lineal para un determinado rango de distancias; encontrando coeficiente de atenuación anelástica  $\gamma = 0.07 \text{ grados}^{-1}$  y las relaciones de magnitud  $mb_{Lg}$  para la componente vertical, para períodos de  $1.0 \pm 0.3$  s.

Bollinger (1973) determina una fórmula tentativa para el cálculo de la magnitud a partir de la fase Lg para la parte sudeste de los Estados Unidos; también determina que el coeficiente  $B = 1.66$  encontrado por Nuttli (1973) varía 0.30 unidades.

TABLA 1

FÓRMULAS PARA DETERMINAR LA MAGNITUD  $mb_{Lg}$

Baker (1970) ESTADOS UNIDOS	$M = \log (A/T) + Q + S$	$Q = a \log \Delta - b$
Sindorf (1972) NORTE DE ESTADOS UNIDOS	$M_{LZ} = \log (A/T) - Q$	
Nuttli (1975) ESTE NORTE AMERICA	$mb_{Lg} = 3.75 + 0.90 (\log \Delta) + \log (A/T)$ $mb_{Lg} = 3.30 + 1.66 (\log \Delta) + \log (A/T)$	$0.5^\circ \leq \Delta \leq 4^\circ$ $4^\circ \leq \Delta \leq 30^\circ$
Bollinger (1973) SUDESTE DE ESTADOS UNIDOS	$mb_{Lg} = -0.10 + 1.66 \log (\Delta) + \log (A/T)$	
Payo y de Miguel (1975) IBERICA	$mb_{Lg} = \log (A/T) + \sigma(\Delta)$	$\sigma(\Delta) = m_0 - f(\Delta)$
Street (1976) NORESTE DE NORTEAMERICA	$mb_{Lg} = 3.75 + 0.90 \log \Delta + \log (A/T)$ $mb_{Lg} = 3.30 + 1.66 \log \Delta + \log (A/T)$	$0.5^\circ \leq \Delta \leq 4^\circ$ $4^\circ \leq \Delta \leq 20^\circ$
Street and Turcotte (1976) NORESTE DE NORTEAMERICA	$mb_{Lg} = MS + 1.2$ $mb_{Lg} = 0.61 MS + 2.33$	$1.8 \leq mb_{Lg} \leq 4.4$ $4.4 \leq mb_{Lg} \leq 6.8$
Nuttli (1980) IRAN	$mb_{Lg} = \log A + 3.62 \log (\Delta) - 4.80$ $mb_{Lg} = \log A + 6.40 \log (\Delta) - 13.15$	$400 \text{ km} \leq \Delta \leq 1000 \text{ km}$ $1000 \text{ km} \leq \Delta \leq 1500 \text{ km}$
Herrmann and Nuttli (1981) ESTE DE NORTEAMERICA	$mb_{Lg} = 3.81 + 0.83 \log (\Delta) + \gamma(\Delta - 0.09) \log e + \log A$	

Donde:  $M, M_{LZ}, mb_{Lg}$  = Magnitud calculada a partir de la fase  $Lg$   
 $A$  = Amplitud máxima de la componente vertical de corto período en micrones ( $\mu$ )  
 $T$  = Período en segundos para la máxima amplitud  
 $\Delta$  = Distancia epicentral en grados  
 $Q$  = Factor de corrección de la distancia  
 $S$  = Factor de corrección por estación  
 $\delta(\Delta)$  = Relación de la atenuación de la amplitud con la distancia  
 $m_0$  = Rango de Magnitud considerada  
 $f(\Delta)$  = Variación de la amplitud con la distancia  
 $MS$  = Momento espectral  
 $\gamma$  = Coeficiente de atenuación anelástica ( $\text{grados}^{-1}$ )

Gonzalo Payo y Fernando de Miguel (1974) determinan una fórmula para el cálculo de magnitudes a partir de la fase Lg, para sismos de la región Ibérica.

Street (1976) estudia la fase Lg para la parte noreste de Norte América, encontrando que  $\gamma$  varía entre 0.10 y 0.12 grados<sup>-1</sup>.

Street and Turcotte (1977), estudiando momentos espectrales de sismos de la parte noreste de Norte América, relacionan el momento espectral (MS) con la magnitud  $mb_{Lg}$ .

Jones et al. (1977) analizan sismos de la parte sudeste de los Estados Unidos, estudian la amplitud de la fase Lg de eventos de magnitud-cero como función de la distancia entre 150 y 850 km, encontrando una dependencia de la atenuación con el azimut de la propagación de las ondas sísmicas.

Bollinger (1979) determina que el coeficiente de atenuación anelástica para Lg en la parte sudeste de Estados Unidos es  $\gamma = 0.07$  grados<sup>-1</sup> para distancia epicentral de 100 a 700 km y para distancias mayores  $\gamma \approx 0.10$  grados<sup>-1</sup>.

Nuttli (1980), estudiando la fase Lg en sismogramas verticales de corto período para sismos de Irán, considerando períodos de un segundo, determina que el valor promedio del coeficiente de atenuación anelástica es igual a  $\gamma = 0.0045$  km<sup>-1</sup>.

Nuttli (1981), usando datos de sismos y explosiones de la parte occidental y central de la Unión Soviética, determina que los coeficientes de atenuación anelástica para la fase Lg de 1 segundo de período son:  $\gamma \approx 0.15$  grados<sup>-1</sup> para las altas tierras del Asia occidental y central y para los caminos cerca del Mar Caspio a las estaciones detrás del borde sur de la Unión Soviética es  $\gamma \approx 0.39$  grados<sup>-1</sup>; comparando la amplitud de Lg con la de la onda P, nota que para Asia central ésta es cerca de 10 veces mayor que la amplitud de P para distancias entre 4° y 8°, hasta ser iguales cerca a los 18°; para el sudeste del Mar Caspio la amplitud de Lg es cerca a 4 veces la amplitud de P para los 4° y alrededor de los 10° es igual.

Herrmann y Nuttli (1982) estudian la relación entre la magnitud local ( $M_L$ ) calculada por Anderson y Wood en 1925 y la magnitud  $mb_{Lg}$  calculada para la fase Lg; determinan que la amplitud ( $A_0$ ) para una distancia de 10° es igual a 115 milimicrones. Postulan una fórmula de magnitud  $mb_{Lg}$  en función de  $\Delta$ . Concluyen que  $mb_{Lg}$  es igual a  $M_L$  para un rango de magnitudes entre 3.0 y 5.0.

## DATOS

Se analizaron 580 sismos ocurridos en/o cerca (a menos de  $1^\circ$  de la costa) de Sudamérica y registrados en la estación sismológica de la Paz-Bolivia (LPB) tipo WWSSN. Los sismos considerados son de 1974 a 1987 con magnitudes  $m_b$  entre 3.8 y 5.8, profundidades de foco ( $h$ ) entre los 0 y 200 kilómetros de profundidad. Los datos sísmicos fueron tomados de los Catálogos y Boletines del International Seismological Centre (ISC).

### CARACTERISTICAS DE LAS ONDAS Lg EN SUDAMERICA

Las ondas Lg son ondas superficiales de corto período, transversales y polarizadas en el plano horizontal; sólo se propagan por la corteza continental. En algunos casos las acompañan otras ondas guiadas, antecediendo las Li y siguiendo las Rg. Por lo general, cuando las Lg están bien desarrolladas, las ondas S están atenuadas (Cabré et al., 1989). Las figuras 1a y 1b muestran las curvas de tiempo de viaje versus distancia para las fases Lg y P. Las Lg presentan velocidades de grupo de  $3.59 \pm 0.012$  km/s para sismos superficiales ( $h < 70$  km) y  $3.65 \pm 0.011$  km/s para sismos intermedios ( $70 \leq h \leq 200$ ).

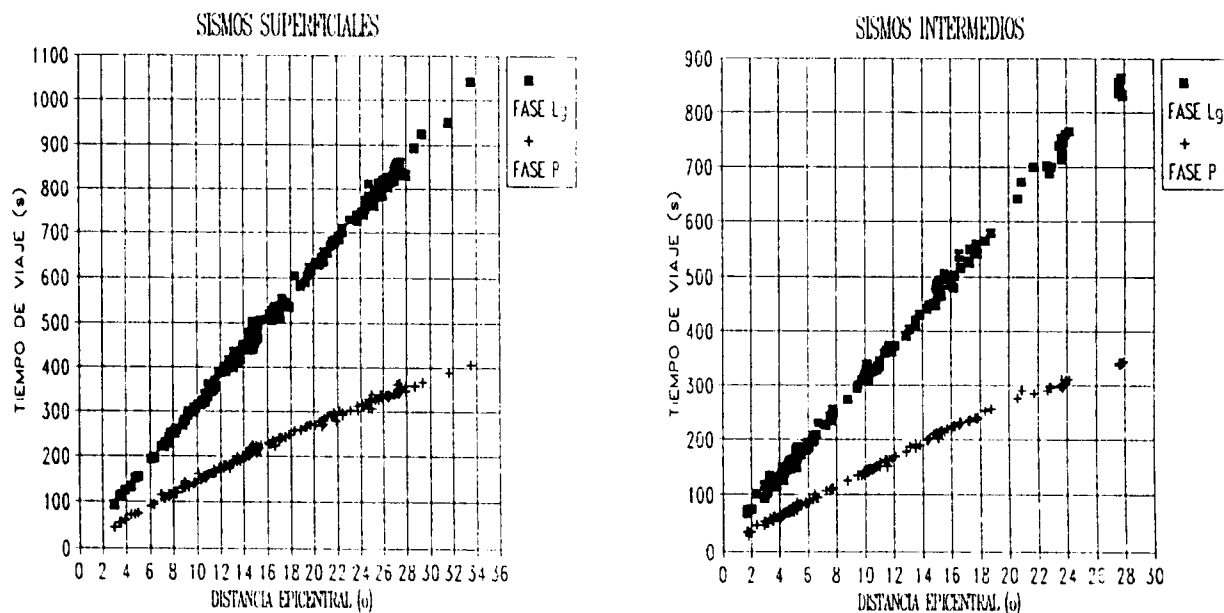


Fig.1. Curvas de tiempo de viaje versus distancia, fases Lg y P.  
1a. Sismos superficiales y 1b. Sismos intermedios.

Considerando el cociente entre la máxima amplitud Lg (en micrones) y P (amplitud máxima en micrones de la fase P de los 5 primeros ciclos) para Sudamérica, Lg/P es mayor a 1 (Cabré et al., 1989). Para muchas regiones de Sudamérica se observan más de una llegada de ondas P con diferentes amplitudes (Cabré et al., 1991).

En relación al origen de los sismos, las Lg presentan las siguientes características (actualizado de Minaya et al., 1987):

Venezuela, Trinidad y Sur del Caribe; las Lg son claras, bien desarrolladas, comienzo impulsivo, algunas veces emergente, interferidas en algunos casos por ondas de corto período (Fig. 3 eventos A y B). Otras fases de ondas guiadas son también notables.

Colombia presenta tanto Lg claras bien desarrolladas, impulsivas, como emergentes y no claras (Fig. 3 evento C). Se pueden distinguir tres regiones; las Lg de la costa oeste y Cordillera occidental están mucho más atenuadas. Para la Cordillera central son más claras pero de comienzos emergentes, mientras que en la parte más oriental (estribaciones de la Cordillera oriental) son claras y de comienzos impulsivos. Presenta Rg en sismos superficiales.

Ecuador; las Lg son de comienzos emergentes, pequeña amplitud (Fig. 3 evento E). En sismos intermedios se distinguen otras fases.

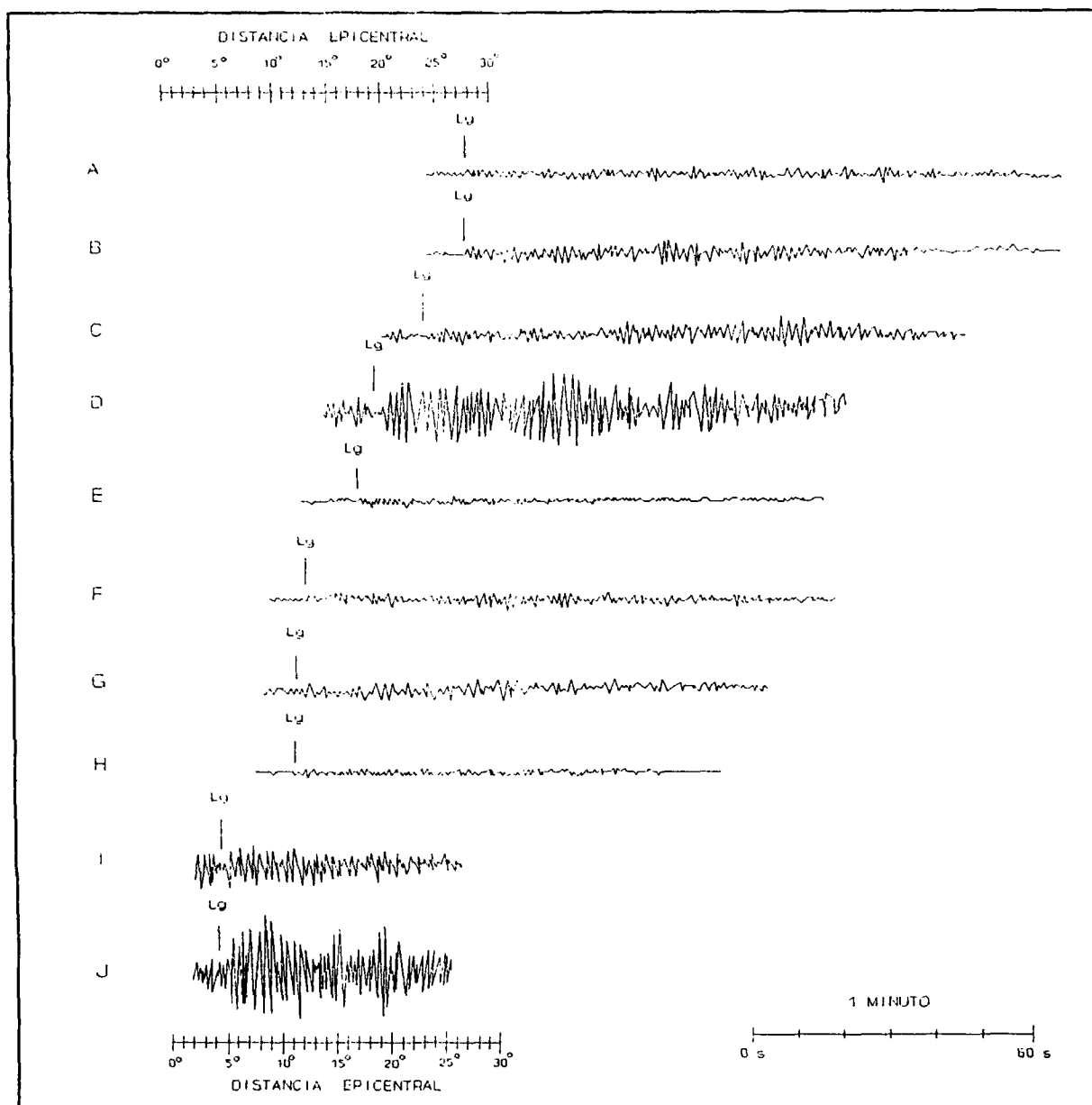
Brasil presenta fases Lg sumamente claras, bien desarrolladas, comienzos impulsivos (Fig. 3 evento D); acompañan otras fases de ondas guiadas claras. Los sismos profundos del Brasil Occidental no presentan Lg.

Argentina; presenta Lg poco claras, comienzos emergentes, de poca amplitud (Fig. 3 evento H); las Lg son una fase simple y con períodos mayores o igual a las Lg de Chile; son de corta duración y no se observan en todos los casos.

Perú y Frontera Perú-Brasil; predominan las Lg claras, bien desarrolladas y de comienzos emergentes independientemente de la distancia (Fig. 3 evento F); en muchos casos presentan ondas Li y Rg claras.

Chile y Frontera Chile-Bolivia; predominan las Lg no claras, poca amplitud y comienzos emergentes (Fig. 3 eventos G y I), presentan mayores períodos que en las otras regiones, excepto Argentina; siempre son una fase simple.

Bolivia presenta en general Lg emergentes y comprimidas (no siempre fáciles de identificar) claras para los sismos de la parte central de Bolivia y menos claras para la Frontera Perú-Bolivia y parte sur de Bolivia (Fig. 3 evento J).



EVENTO	REGION	FECHA			h (km)	mb	$\Delta$ (°)	Az (°)	COMPONENTE
		A	M	D					
A	Venezuela	82	VIII	10	104	4.8	27.59	12	N-S
B	Costa de Venezuela	79	VII	17	40	4.6	27.24	13	N-S
C	Colombia	83	VIII	29	169	5.0	23.67	348	E-W
D	Brasil	76	II	22	10	4.8	18.96	28	N-S
E	Ecuador	81	V	26	107	5.1	17.29	258	E-W
F	Perú	82	VIII	12	33	4.7	12.35	323	N-S
G	Costa Norte Chile	72	V	28	53	4.8	11.87	195	N-S
H	Argentina	76	I	04	48	4.8	11.47	175	E-W
I	Frontera Chile-Bolivia	79	I	24	128	4.6	4.95	186	N-S
J	Bolivia	79	II	15	51	4.8	4.79	115	N-S

Fig. 3. Registros de las componentes horizontales de corto período de la estación LPB, mostrando los arribs de las Lg y sus respectivas distancias epicentrales en grados, para diferentes azimuts (Az = Azimut estación-epicentro).



## PROCEDIMIENTO

Se leyeron los datos de las máximas amplitudes  $A$  (micrones) y sus correspondientes períodos  $T$  (segundos) para la fase  $L_g$  (predominan los períodos entre 1.1 y 1.3 s) de los sismogramas horizontales analógicos de corto período (debido a que presentan mayor desarrollo en las componentes horizontales) de la estación sismológica LPB, dividiéndolos de acuerdo a la trayectoria en dos regiones: Cordillera (Cordillera de los Andes, parte sur al nor-oeste de Sudamérica) y Escudo (parte norte, Escudo de Guayana y parte este, Escudo Brasileiro), y separándolos según la profundidad.

Considerando la fórmula general de magnitudes para  $L_g$  (1):

$$mb_{L_g} = B + C (\log \Delta) + \log (A/T) \quad (1)$$

primeramente se determinó el coeficiente  $C$ , mediante un ajuste lineal entre  $\log (A/T)$  versus  $\log \Delta$ , mediante mínimos cuadrados, para diferentes rangos de magnitud  $mb$ , realizando sucesivos ajustes se obtuvo un valor promedio de  $C$  y  $B_1$ :

$$\log (A/T) = B_1 + C \log(\Delta) \quad (2)$$

seguidamente se ajustó  $\log (A/T)$  versus  $mb$  para una pendiente igual a la unidad.

$$\log (A/T) = B_2 + mb \quad (3)$$

siendo el coeficiente  $B = B_1 + B_2$

Reemplazando los coeficientes  $B$  y  $C$  en la fórmula (1), se obtuvieron las relaciones  $mb_{L_g}$ , para las regiones de Cordillera y de Escudo para Sudamérica.

### SISMOS SUPERFICIALES

CORDILLERA	$mb_{L_g} = 3.70 + 2.19 (\log \Delta) + \log (A/T)$	$\Delta < 18^\circ$	(4)
------------	---	---------------------	-----

ESCUDO	$mb_{L_g} = 4.40 + 1.12 (\log \Delta) + \log (A/T)$	$10^\circ < \Delta \leq 34^\circ$	(5)
--------	---	-----------------------------------	-----

### SISMOS INTERMEDIOS

CORDILLERA	$mb_{L_g} = 3.80 + 1.97 (\log \Delta) + \log (A/T)$	$\Delta < 18^\circ$	(6)
------------	---	---------------------	-----

ESCUDO	$mb_{L_g} = 4.50 + 1.18 (\log \Delta) + \log (A/T)$	$20^\circ < \Delta \leq 28^\circ$	(7)
--------	---	-----------------------------------	-----

Donde:  $\Delta$  = Distancia epicentral en grados  
 $A$  = Máxima amplitud de la fase  $L_g$  (componente horizontal de corto período) en micrones  
 $T$  = Período de la máxima amplitud en segundos

La Tabla 2 muestra diferentes rangos de magnitudes  $mb$  calculadas por el ISC ( $mb$ ) y las desviaciones standard de  $mb - mb_{L_g}$  ( $mb_{L_g}$  magnitud calculada a partir de la fase  $L_g$ , empleando las relaciones: (4), (5), (6) y (7), para sismos sudamericanos).

TABLA 2

DESVIACIONES STANDARD ENTRE  $mb$  Y  $mb_{Lg}$  PARA SUDAMÉRICA

mb	$mb - mb_{Lg}$			
	SISMOS SUPERFICIALES		SISMOS INTERMEDIOS	
	CORDILLERA $\Delta < 18^\circ$	ESCUDO $10^\circ < \Delta \leq 34^\circ$	CORDILLERA $\Delta < 18^\circ$	ESCUDO $20^\circ < \Delta \leq 28^\circ$
$mb \leq 4.0$	0.12		0.19	
$4.1 \leq mb \leq 4.5$	0.25	0.18	0.24	0.25
$4.6 \leq mb \leq 5.0$	0.24	0.24	0.25	0.24
$5.1 \leq mb \leq 5.5$	0.22	0.25	0.23	0.23
$5.6 \leq mb \leq 6.0$	0.22	0.16	0.17	0.05
$mb = 6.4$	0.35			

Usando la relación empleada de la amplitud de las ondas superficiales dispersadas, en el dominio del tiempo, para una fuente de ondas elásticas, en una Tierra esférica, Nuttli (1973):

$$A = A_0 * (\Delta * \sin(\Delta))^{-\alpha} * \exp^{-\gamma \Delta} \quad (8)$$

Donde:  $A_0$  es la amplitud de la onda en el origen,  $A$  = máxima amplitud de la fase  $Lg$ ,  $\Delta$  = distancia epicentral en grados,  $\alpha$  = coeficiente de la atenuación debido al esparcimiento geométrico (en este caso  $\alpha = 0.5$ ) y  $\gamma$  = coeficiente de atenuación anelástica; utilizando la relación (8) se obtuvieron los valores medios del coeficiente de atenuación anelástica:  $\gamma = 0.20 \pm 0.03$  grados<sup>-1</sup> para la Cordillera de los Andes y  $\gamma = 0.09 \pm 0.04$  grados<sup>-1</sup> para el Escudo.

### CONCLUSIONES

En general las magnitudes  $mb$  y  $mb_{Lg}$  son aproximadamente iguales ( $mb - mb_{Lg} \leq \pm 0.25$ ) para sismos de la Cordillera ( $\Delta < 18^\circ$ ) para un rango de magnitudes  $4.0 \leq mb \leq 6.0$  y para el Escudo entre  $4.1 < mb \leq 6.0$  ( $10^\circ \leq \Delta \leq 34^\circ$ ). Para magnitudes  $mb < 4.0$  las  $mb_{Lg}$  son ligeramente mayores y para  $mb > 6.0$  son ligeramente menores.

Las relaciones obtenidas  $mb_{Lg}$  para las regiones de Cordillera (4) y (6) y de Escudo (5) y (7) son similares, debido a que las  $Lg$  son ondas S atrapadas y convertidas en ondas SH en la corteza continental.

Realizando una ponderación de los resultados, se obtienen dos fórmulas generales consistentes, para las magnitudes  $mb_{Lg}$  para sismos sudamericanos.

$$\text{CORDILLERA} \quad mb_{Lg} = 3.80 + 2.00 (\log \Delta) + \log (A/T) \quad \Delta < 18^\circ \quad (9)$$

$$\text{ESCUDO} \quad mb_{Lg} = 4.40 + 1.15 (\log \Delta) + \log (A/T) \quad 10^\circ < \Delta \leq 34^\circ \quad (10)$$

Donde:  $\Delta$  = Distancia epicentral en grados  
 $A$  = Máxima amplitud de la fase  $Lg$  ( $\mu$ )  
 (componente horizontal de corto período)  
 $T$  = Período para la máxima amplitud (s)

Las desviaciones standard para las relaciones (9) y (10) son: 0.21 y 0.22 respectivamente.

Para los rangos de distancia considerados, la relación entre los  $(A/T)$  versus  $\log(\Delta)$  se satisface con un ajuste de tipo lineal. Se encuentran diferencias entre las fórmulas de magnitud  $mb_{Lg}$  para Sudamérica y otras regiones; los valores de  $C$  para el Escudo son aproximadamente iguales a los calculados por Nuttli (1973) y Street (1976), para la parte este y noreste de Norteamérica; la diferencia entre los valores de  $B$ , son debidos al umbral de detectabilidad de la estación LPB (el cual es mayor) y además varían en relación inversamente proporcional con  $C$ ; mientras que para la Cordillera de los Andes los valores de  $C$  son mucho mayores, lo que indica una mayor atenuación de las ondas sísmicas; esto se confirma también con los valores de  $\gamma$  calculados, siendo  $B$  directamente proporcional a  $\gamma$ .

Las magnitudes  $mb_{Lg}$  constituyen una buena alternativa para sismos superficiales e intermedios, con magnitudes  $4 \leq mb \leq 6.0$ , para las regiones de la Cordillera de los Andes y de Escudo.

#### AGRADECIMIENTOS

Deseo expresar mis agradecimientos al Dr. Ramón Cabré S.J. por sus comentarios y revisión a este estudio, como también al Geophysics Laboratory, Air Force Systems Command, USAF, bajo el Grant AFOSR-89-0532 B, quienes han auspiciado el presente trabajo.

# BIBLIOGRAFIA

- Baker, R. G. (1967). Preliminary study for determining magnitude from Lg, *Earthquakes Notes*, **38**, 23-28.
- Baker, R. G. (1970). Determining magnitude from Lg, *Bull. Seism. Soc. Am.*, **60**, 1907-1919.
- Bath, M. (1979). Introduction to Seismology. Birkhäuser Verlag Basel, Boston, Stuttgart.
- Bollinger G. A. (1973). Seismicity of the southeastern United States, *Bull. Seism. Soc. Am.*, **63**, 1785-1808.
- Bollinger G. A. (1979). Attenuation of the Lg Phase and the determination of mb in the Southeastern United States, *Bull. Seism. Soc. Am.*, **69**, No. 1, 45-63.
- Cabré, R. S. J., Minaya, E., Alcócer, I. and Ayala, R. (1989). Propagation and Attenuation of Lg waves in South America, *Final Report, Geophysics Laboratory, Air Force Systems Command, United States Air Force*. AFGL-TR-89-0273, ADA218853
- Cabré, R. S.J., Minaya, E., Ayala, R. and M. Capriles (1991). Lg and other Regional Phases in South America, *Annual Report, Geophysics Laboratory*, PL-TR-92-2008, ADA248375
- Evernden, J. F. (1967). Magnitude determinations at regional and near regional distance in the United States, *Bull. Seism. Soc. Am.*, **57**, 591-639.
- Evernden, J. F., W. J. Best, P. W. Pomeroy, T. V. McEvelly, J. M. Savino and L. R. Sykes (1971). Discrimination between small-magnitude earthquakes and explosions, *J. Geophys. Res.*, **76**, 8042-8055.
- Freemann, H. W. (1969). Estimating earthquake magnitude, *Bull. Seism. Soc. Am.*, **57**, 4, 747-760.
- Herrmann, R. B. and O. W. Nuttli (1982). Magnitude: the relation of  $M_L$  to  $mb_{Lg}$ , *Bull. Seism. Soc. Ame.*, **72**, 384-397.
- Jones, F. B., L. T. Long and J. H. Mckee (1977). Study of the attenuation and azimuthal dependence of seismic wave propagation in the southeastern United States, *Bull. Seism. Soc. Am.*, **67**, 1503-1513.
- Minaya, E., Ayala, R., Alcócer, I. y R. Cabré S.J. (1989). Ondas Lg de Sismos Sudamericanos, *Revista de Geofísica*, No. 31, IPGH.
- Nuttli, O. W. (1973). Magnitude relations for eastern North America, *J. Geophys. Res.*, **78**, No. 5, 876-885.
- Nuttli, O. W. (1980). The excitation and attenuation of seismic crustal phases in Iran, *Bull. Seism. Soc. Ame.*, **70**, No. 2, 469-485.
- Nuttli, O. W. (1981). On the attenuation of Lg waves in the western and central Asia and their use as a discriminant between earthquakes and explosions, *Bull. Seism. Soc. Amer.*, **71**, 249-261.
- Payo, G. y F. de Miguel (1974). Magnitud de los sismos de la región Ibérica a partir de la fase Lg, *Revista Geofísica*, Vol. XXXII, No. 3 y 4, 159-174.
- Richter, C. F. (1935). An instrumental earthquake magnitudes scale, *Bull. Seism. Soc. Am.*, **25**, 1-32.

- Richter, C. F. (1958). Elementary Seismology. W. H. Freeman, San Francisco, California.
- Sindorf, J. G. (1972). Determining magnitude values from the Lg phase from short-period vertical seismographs. *Earthquakes Notes* 39, 20-32.
- Street R. L. (1976). Scaling northeastern United States/southeastern Canadian earthquakes by their Lg waves, *Bull. Seism. Soc. Am.*, 66, 1525-1537.
- Street, R. L. and F. T. Turcotte (1977). A study of northeastern North America spectral moments. Magnitudes and Intensities, *Bull. Seism. Soc. Am.*, 67, 599-614.

**ANNEX 2**

# ATENUACION DE LAS INTENSIDADES SISMICAS EN LA CORDILLERA DE LOS ANDES CENTRALES, BOLIVIA

R. RODOLFO AYALA SÁNCHEZ \*

## RESUMEN

Se analizaron los sismos bolivianos sentidos, localizados en la Cordillera de los Andes Centrales, a partir de los datos macrosísmicos. Nueve relaciones de atenuación de las intensidades sísmicas con la distancia, fueron derivadas para Bolivia, usando la ecuación general:

$$I(D) = I_0 + a + b \log D + c D$$

donde  $I_0$  es la intensidad máxima,  $I(D)$  es la intensidad a la distancia  $D$  (km) desde el hipocentro y  $a$ ,  $b$ ,  $c$  son parámetros apropiados para cada una de las nueve zonas. También se determinaron las relaciones entre  $I_0$  y  $m_b$ . En general la máxima atenuación sigue la dirección perpendicular a las estructuras geológico-tectónicas. Se distinguen cuatro zonas geológico-tectónicas (relacionadas a varias fuentes sísmogénicas) de diferente atenuación sísmica, de menor a mayor atenuación, que son: la primera y con la menor atenuación relacionada con la Cordillera Oriental norte (sismos de Consata); la segunda zona entre el Subandino central y las Llanuras Chaco-Benianas (sismos de Santa Cruz); la tercera relacionada a cuencas sedimentarias cuaternarias de la parte central de la Cordillera Oriental (sismos de Arque, Quiroga, Tiquipaya, Sucre) y los sismos de Tupiza con una gran atenuación con la profundidad; y la cuarta zona correspondiente al Subandino central (sismos de Chapare) y Subandino sur (sismos de Yacuiba).

## ABSTRACT

The bolivian earthquakes felt, located in the Central Andean Cordillera were analysed. Nine relations of attenuation of the seismic intensities with the distance were derived for Bolivia, using the general equation:

$$I(D) = I_0 + a + b \log D + c D$$

where  $I_0$  is the maximum intensity,  $I(D)$  is the intensity at the distance  $D$  (km) from the hypocenter and  $a$ ,  $b$ ,  $c$  are appropriate parameters for each of the nine zones. The relations between  $I_0$  and  $m_b$  were determined too. Generally the maximum attenuation is in direction perpendicular to the geological-tectonic structures. There are four zones tectonic-geological (related to many sismogenic sources) of different seismic attenuation, from less to high attenuation, they are: the first with the least attenuation related to north Eastern Cordillera (earthquakes of Consata); the second zone between the central Subandean and Chaco-Benian Plains (earthquakes of Santa Cruz); the third related to quaternary sedimentary basins of the central part of the Eastern Cordillera (earthquakes of Arque, Quiroga, Tiquipaya, Sucre) and the earthquakes of Tupiza with a high attenuation with the depth and the fourth corresponding to central Subandean (earthquakes of Chapare) and south Subandean (earthquakes of Yacuiba).

## INTRODUCCION

Bolivia es un país con sismicidad baja a moderada, pero en el pasado grandes sismos afectaron diferentes zonas de Bolivia, correspondientes a la región de los Andes Centrales, entre ellos podemos citar los más importantes: Noviembre 10 de 1965 sentido con intensidad VIII en Sucre, Noviembre 26 de 1884 con intensidad VIII en Tarabuco; Noviembre 23 de 1887 y Marzo 23 de 1899 con intensidad IX en Yacuiba y Campo Grande; Febrero 24 de 1947 con intensidad VIII en Consata y Agosto 26 de 1957 con intensidad VII en Postrervalle. Los sismos bolivianos sentidos son mostrados en el Mapa de distribución de epicentros (Fig. 1).

\* Observatorio San Calixto, La Paz, Bolivia.

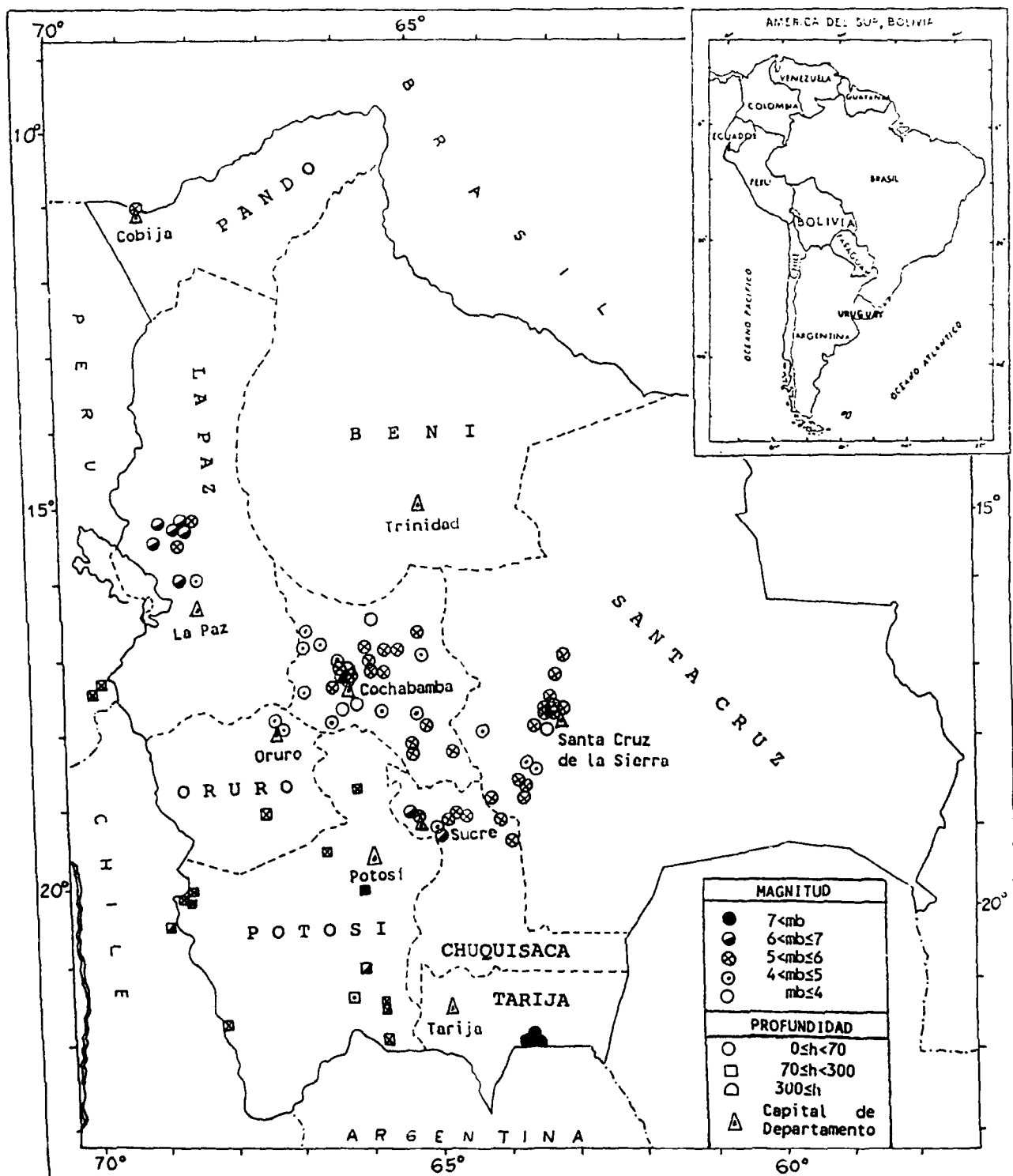


FIG. 1. Mapa de Distribución de epicentros de los sismos bolivianos sentidos desde 1647 a 1988, de acuerdo a magnitud y profundidad; y división política de Bolivia mostrando los Departamentos y las Capitales de Departamento.



## DATOS

Los datos macrosísmicos correspondientes a los sismos bolivianos de la región de los Andes Centrales fueron tomados de los Catálogos de Terremotos para América del Sur: Bolivia - Brasil (CERESIS, 1985); Catálogo de Sismos de Perú y Bolivia (Ocola, 1982); Historia Sísmica de Bolivia (Descotes y Cabré, 1960) y los reportes del NEIC (National Earthquake Information Center), de los Catálogos de Terremotos del ISC (International Seismological Centre); los datos considerados corresponden a los años de 1647 a 1988 (Tabla 1).

En contados casos donde no existen datos de magnitud, profundidad de foco ( $h$ ) o intensidad máxima, éstas fueron estimadas (ver Tabla 1, en ésta las profundidades no expresadas se supone que son superficiales). Para los datos de intensidades sísmicas fue considerado un error de  $\pm 0.2$  unidades (escala de Mercalli Modificada).

## ANALISIS

Las relaciones de las intensidades sísmicas con la distancia fueron estudiadas por Karnik (1969), Howell (1974), Howell and Schultz (1975), Gupta and Nuttli (1976), Chandra et al. (1979), Minaya (1985), usando la siguiente ecuación general:

$$I(\Delta) = I_0 + a + b \Delta + c \log \Delta \quad (1)$$

Donde  $I(\Delta)$  es la intensidad sísmica a la distancia  $\Delta$  desde el epicentro,  $I_0$  es la intensidad epicentral (intensidad máxima) y  $a$ ,  $b$ ,  $c$ , son parámetros apropiados para cada zona;  $a$  es definida como una función de la profundidad focal ( $h$ ),  $b$  es el coeficiente relacionado al esparcimiento geométrico y  $c$  está relacionada al coeficiente de absorción.

Debido a que existe una variación en la profundidad de los sismos sentidos, se vio por conveniente utilizar la distancia hipocentral  $D$ .

$$D = (\Delta^2 + h^2)^{1/2} \quad (2)$$

Reemplazando (2) en (1), se obtiene la ecuación general:

$$I(D) = I_0 + a + b D + c \log D \quad (3)$$

Para determinar las relaciones entre  $I_0$  y la magnitud calculada por las ondas de cuerpo ( $mb$ ), se utilizó la fórmula basada en la relación empírica dada por Gutenberg y Richter (1956):

$$I_0 = a_1 mb + e_1 \quad (4)$$

Donde  $a_1$  y  $e_1$  son apropiadas constantes para cada zona.

Reemplazando (4) en (3), se obtuvo la relación de la atenuación de las intensidades sísmicas con la distancia para diferentes magnitudes  $mb$ :

$$I(D) = a_1 mb + a_2 + b D + c \log D \quad (5)$$

Donde:

$$a_2 = a + e_1 \quad (6)$$

Los coeficientes  $a$ ,  $b$ ,  $c$ ,  $a_1$ ,  $a_2$  y  $e_1$  fueron calculados usando el procedimiento de ajuste por mínimos cuadrados.

TABLA 1

SISMOS BOLIVIANOS SENTIDOS DE ACUERDO A LA DIVISION POR DEPARTAMENTOS

FECHA			HORA ORIGEN			LATITUD	LONGITUD	h	mb	Io	LOCALIDAD	DEPARTAMENTO	OBSERVACIONES
A	M	D	H	M	S	° S	° W	km		(MM)			
1919	05	05	18	30	28	11.02	68.77	-	5.3	VII	Cobija	PANDO	
1647	00	00	00	00	00	16.10	68.05	-	4.8	V	Zongo	LA PAZ	
1877	05	17	00	00	00	15.33	68.54	55	6.3	VII	Consata	LA PAZ	
1891	08	15	11	02	00	15.33	68.54	20	6.2	VII	Consata	LA PAZ	
1896	07	06	11	02	00	15.33	68.54	30	6.2	VII	Consata	LA PAZ	
1920	07	13	06	34	06	15.30	68.35	-	5.6	V	Consata-Mapiri	LA PAZ	
1923	09	02	22	38	12	16.00	68.50	-	6.1	III	Consata-Mapiri	LA PAZ	
1937	11	03	06	06	00	15.50	68.50	33	5.4	VI	Villa Guachalla	LA PAZ	
1947	02	24	17	31	36	15.50	68.80	65	6.8	VIII	Consata	LA PAZ	Caída de rocas
1956	08	23	13	48	26	15.27	68.67	33	5.2	VI	Consata	LA PAZ	
1983	01	01	05	31	51.9	17.22	69.25	145	5.6	II	La Paz	FRONTERA BOLIVIA-PERU	
1983	09	01	20	01	42.8	17.44	69.66	73	5.9	II	La Paz	FRONTERA BOLIVIA-PERU	
1931	03	17	00	55	10	17.97	67.14	-	4.3	V	Oruro ciudad	ORURO	
1982	08	23	16	26	2.9	17.90	67.10	20	4.7	V	Oruro ciudad	ORURO	
1986	03	15	11	29	39.0	19.07	67.44	98	5.6	III	Cochabamba	ORURO	
1871	02	23	06	30	00	16.72	65.12	-	4.9	VI	San Antonio	COCHABAMBA	
1909	07	23	12	15	00	17.43	66.35	-	5.0	VI	Sipe-Sipe	COCHABAMBA	
1914	05	07	10	21	34.9	17.18	65.86	-	5.2	IV	Cochabamba ciudad	COCHABAMBA	
1920	12	22	05	53	44	16.97	65.85	-	5.3	V	Cochabamba ciudad	COCHABAMBA	
1925	10	25	04	31	09	18.20	65.17	-	5.2	VI	Aiquile	COCHABAMBA	
1926	11	13	00	17	31.3	17.40	66.10	-	5.4	VI	Sipe-Sipe	COCHABAMBA	
1928	07	06	04	24	05	17.24	66.29	-	5.3	VI	Cochabamba ciudad	COCHABAMBA	
1942	12	25	08	00	28	17.28	65.81	-	5.7	VI	Cochabamba ciudad	COCHABAMBA	
1943	02	18	15	38	46	17.38	66.19	-	5.2	VI	Cochabamba ciudad	COCHABAMBA	
1948	05	01	18	46	49	17.78	65.19	-	4.4	IV	Cochabamba ciudad	COCHABAMBA	
1950	11	02	06	18	02.8	17.38	66.19	-	5.3	V	Tiquipaya	COCHABAMBA	
1958	01	06	16	53	00	18.31	64.67	-	5.2	VI	Pasorapa	COCHABAMBA	
1958	09	01	14	30	46	18.00	65.00	-	5.9	VII	Cochabamba ciudad	COCHABAMBA	
1959	10	19	14	29	44	17.38	66.19	-	5.4	VI	Cochabamba ciudad	COCHABAMBA	
1962	09	15	23	55	03	17.78	66.31	-	3.4	IV	Cochabamba ciudad	COCHABAMBA	
1964	01	05	23	38	19.9	17.65	66.03	-	2.0	III	Tiquipaya	COCHABAMBA	
1972	05	12	17	16	28	17.46	66.87	43	4.9	VII	Tiquipaya	COCHABAMBA	
1976	02	22	08	09	22	18.33	65.35	41	5.2	VII	Quiroga	COCHABAMBA	
1976	06	30	17	16	59	17.91	66.38	33	4.8	V	Arque	COCHABAMBA	Caída de rocas
1981	04	05	12	17	29	17.22	66.23	43	4.3	IV	Tiquipaya	COCHABAMBA	
1981	07	23	13	51	26	17.03	65.11	38	5.1	VII	Chimore	COCHABAMBA	Licuefacción
1983	05	19	08	33	19.4	17.61	65.79	15	4.8	V	Norte de Potosí	COCHABAMBA	
1984	01	16	22	29	58.4	16.52	65.78	21	3.9	IV	Cochabamba ciudad	COCHABAMBA	
1984	03	09	23	56	35.1	16.82	66.70	14	4.4	V	Recoleta	COCHABAMBA	
1985	10	27	04	37	29.5	16.90	66.96	33	4.0	IV	Independencia	COCHABAMBA	
1986	03	20	00	43	26.8	17.10	65.39	52	4.9	IV	Cochabamba ciudad	COCHABAMBA	
1986	05	09	16	23	48.8	17.17	65.62	13	5.6	IV	Cochabamba ciudad	COCHABAMBA	
1986	06	19	20	33	17	16.97	65.49	19	5.3	IV	Cochabamba ciudad	COCHABAMBA	
1986	06	19	21	57	25	16.96	65.46	23	5.4	IV	Cochabamba ciudad	COCHABAMBA	
1845	02	14	00	00	00	17.78	63.17	-	5.4	VI	Santa Cruz de la Sierra	SANTA CRUZ	
1890	11	15	00	00	00	17.78	63.17	-	5.4	VI	Santa Cruz de la Sierra	SANTA CRUZ	
1906	08	17	00	00	00	17.90	63.40	20	5.5	VI	Santa Cruz de la Sierra	SANTA CRUZ	
1913	12	13	22	45	00	17.78	63.17	-	5.4	VI	Santa Cruz de la Sierra	SANTA CRUZ	
1914	02	18	23	30	00	17.78	63.17	-	6.0	VII	Santa Cruz de la Sierra	SANTA CRUZ	
1914	02	20	12	50	00	17.78	63.17	-	4.6	V	Santa Cruz de la Sierra	SANTA CRUZ	
1914	02	22	09	35	00	17.78	63.17	-	6.0	VII	Santa Cruz de la Sierra	SANTA CRUZ	
1929	02	18	00	00	00	17.00	63.00	-	5.5	VI	El Carmen	SANTA CRUZ	
1930	10	20	00	00	00	17.20	63.10	-	5.5	VI	La Esperanza	SANTA CRUZ	
1949	11	07	20	59	52	18.56	63.50	-	5.0	VI	Florida	SANTA CRUZ	
1957	08	26	11	28	52	18.74	63.73	-	6.0	VII	Postrervalle	SANTA CRUZ	Licuefacción
1981	08	23	08	22	51	18.02	64.22	33	4.2	IV	Lagunillas	SANTA CRUZ	
1985	03	19	10	28	35	18.63	63.56	19	5.4	V	Monteagudo	SANTA CRUZ	2 muertos
1985	03	19	10	37	14.6	18.46	63.51	33	4.9	V	Monteagudo	SANTA CRUZ	
1985	03	22	14	02	43	18.63	63.56	9	5.4	V	Santa Cruz de la Sierra	SANTA CRUZ	
1986	08	31	14	24	35	17.91	63.30	-	5.2	V	La Guardia	SANTA CRUZ	
1987	08	22	06	29	17.9	17.94	63.30	33	3.1	III	Santa Cruz de la Sierra	SANTA CRUZ	
1987	02	04	13	30	00	17.78	63.17	-	3.0	III	Warnes	SANTA CRUZ	
1988	08	22	06	29	17.9	17.94	63.30	33	2.0	III	Santa Cruz de la Sierra	SANTA CRUZ	
1650	11	10	16	00	00	19.04	65.26	-	5.8	VIII	Sucre	CHUQUISACA	
1873	02	22	05	45	00	19.10	64.70	-	5.5	V	Sucre	CHUQUISACA	
1884	11	17	03	10	00	19.18	64.87	20	4.8	V	Sucre	CHUQUISACA	
1884	11	26	00	00	00	19.17	64.91	-	6.8	VIII	Tarabuco	CHUQUISACA	
1948	03	27	01	30	07	19.04	65.26	-	6.0	VII	Yotala	CHUQUISACA	1 muerto
1951	06	28	03	07	46	19.30	63.80	-	6.2	V	Sucre	CHUQUISACA	
1957	03	09	22	19	17	19.00	64.00	-	5.3	III	Sucre	CHUQUISACA	
1957	08	26	18	22	18	19.00	68.00	33	6.2	V	Sucre	CHUQUISACA	
1958	06	01	19	47	05	19.00	64.53	-	5.5	V	Aiquile	CHUQUISACA	
1986	01	14	13	13	17.4	18.6	64.03	33	5.1	V	Sucre	CHUQUISACA	
1851	07	05	12	00	00	19.75	65.58	250	7.3	VII	Potosí ciudad	POTOSI	
1909	05	17	08	02	54	20.00	66.00	250	8.2	VIII	Tupiza	POTOSI	
1919	12	28	18	46	44	21.43	65.72	250	5.3	V	Potosí ciudad	POTOSI	
1932	12	25	12	32	03	18.69	66.01	250	5.4	VI	Potosí ciudad	POTOSI	
1951	11	07	22	07	55	21.75	68.00	120	5.9	V	Potosí ciudad	FRONTERA BOLIVIA-CHILE	
1953	10	27	18	20	47	19.50	66.50	200	5.6	VI	Sucre	POTOSI	
1957	11	29	22	19	38	21.00	66.00	250	7.0	VI	Tupiza	POTOSI	
1959	12	22	00	00	00	21.43	65.72	250	5.4	VI	Tupiza	POTOSI	
1960	04	06	02	05	06	20.00	68.50	130	5.0	IV	Potosí ciudad	FRONTERA BOLIVIA-CHILE	
1972	10	10	22	42	48.5	20.09	68.73	127	5.5	V	Oruro ciudad	FRONTERA BOLIVIA-CHILE	
1976	11	30	02	21	12.8	20.14	68.60	92	5.2	V	Oruro ciudad	FRONTERA BOLIVIA-CHILE	
1976	11	30	00	40	56.5	20.57	68.93	70	6.5	VI	Sudeste de Bolivia	FRONTERA BOLIVIA-CHILE	
1978	10	27	10	06	43.1	21.98	65.82	254	5.6	III	Antofagasta (Chile)	POTOSI	
1979	08	10	01	28	39.4	21.33	66.56	226	5.0	III	Sur de Potosí	POTOSI	
1887	09	23	00	00	00	22.03	63.70	-	7.8	IX	Yacuiba	TARIJA	Heridos
1899	03	23	18	00	00	21.97	63.67	-	7.9	IX	Campo Grande	TARIJA	
1973	10	25	14	08	58.5	21.96	63.65	517	6.1	III	Campo Grande	TARIJA	

• Datos estimados por el autor

## GEOLOGIA Y TECTONICA

Bolivia corresponde a tres grandes unidades geológico-tectónicas, que son: la Cordillera de los Andes Centrales, las Llanuras Chaco-Benianas y el Escudo Brasileiro; éstas a su vez están divididas en 7 provincias geológicas (ver Fig. 2): Cordillera Occidental, Altiplano, Cordillera Oriental, Subandino, Llanuras Chaco-Benianas, Serranías Chiquitanas y el Escudo Brasileiro.

Cordillera Occidental consiste principalmente de rocas volcánicas y mesetas volcánicas; Cordillera Oriental norte, está compuesta por rocas paleozoicas (Consata) y grandes cuerpos graníticos, al centro y sur formada por rocas de edad ordovícica (Cordillera centro Oriental), en su parte central presentan cuencas sedimentarias de edad cuaternaria (Arque, Tiquipaya, Quiroga, Sucre), similar al sur (Tupiza, Cordillera de Chichas); las estribaciones de la Cordillera Oriental se denominan Subandino, compuesto principalmente por rocas sedimentarias de edad paleozoica, fuertemente falladas y fracturadas (Yacuiba); al extremo este del Subandino norte y central se presentan depósitos terciarios de pie de monte (Chapare). El Altiplano es una alta meseta correspondiente a una fosa tectónica levantada, de edad mesozoica; está localizado entre las Cordilleras Occidental y Oriental, rellena con rocas sedimentarias de edades desde el paleozoico al terciario y cubiertas por depósitos cuaternarios (Oruro).

Las Llanuras Chaco-Benianas son planicies, con rocas cámbricas, cubiertas por depósitos cuaternarios aluviales (Cobiya y Santa Cruz de la Sierra); a lo largo del Río Beni el basamento precámbrico está cubierto sólo por rocas terciarias. Las Serranías Chiquitanas están compuestas por las más viejas rocas precámbricas en Bolivia, localizadas en las llanuras orientales.

El Escudo Brasileiro está compuesto por rocas precámbricas, que forman la base del continente sudamericano; la parte aflorante en Bolivia se denomina Escudo de Guaporé.

Tectónicamente Bolivia está sobre la Placa tectónica de Sudamérica y sometida a esfuerzos tectónicos debidos a la subducción de la Placa de Nazca; estos esfuerzos originan los grandes lineamientos y fallas; los rumbos de los planos de falla son paralelos (en su mayoría) y perpendiculares al eje de la Cordillera de los Andes Centrales. La mayoría de los sismos bolivianos sentidos están asociados a fallas superficiales (ver Fig. 2), las zonas de Tupiza, frontera con Chile y la frontera con Perú presentan sismos de profundidad intermedia. La zona sureste de Bolivia presenta principalmente sismos profundos, pero los sismos destructores de Yacuiba son asociados con fallas superficiales.

## RESULTADOS

Analizando los Mapas: Distribución de sismos bolivianos sentidos, Geológico-Tectónico simplificado y Areas de Máximas Intensidades Observadas (Minaya, 1985), para este estudio, en relación a los mayores sismos (ver Fig. 3) se consideraron once fuentes sismogénicas (zonas donde los sismos presentan un origen común y están asociados a una única estructura geológica) No se consideraron las zonas de las fronteras con las Repúblicas del Perú y Chile porque se tienen escasos datos macrosísmicos y son de menor importancia. El nombre de cada fuente se tomó de la localidad más importante dentro del área de epicentros. La parte central de Bolivia (Departamento de Cochabamba) fue dividida en cuatro fuentes sismogénicas (basado en Minaya, 1985).

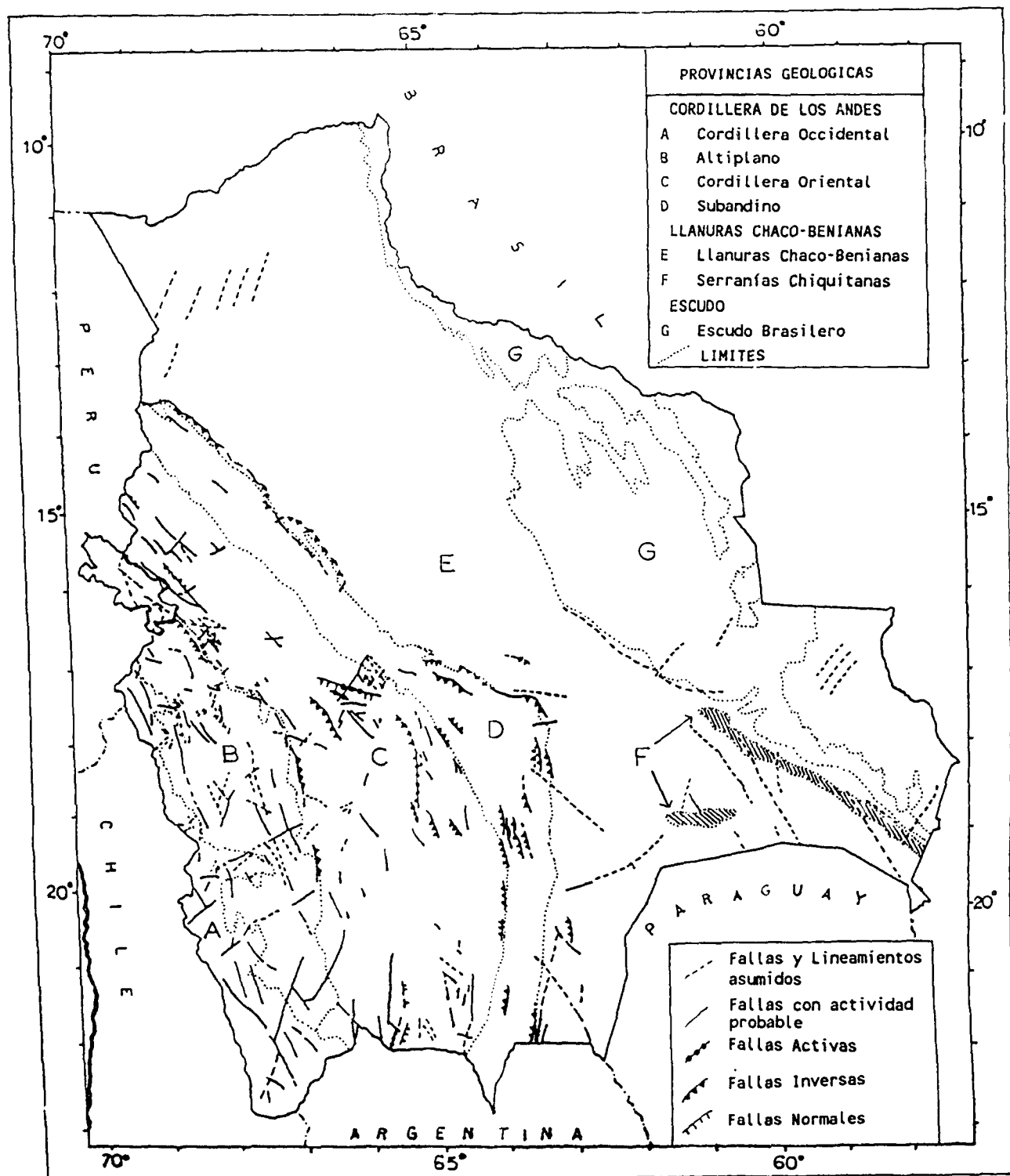


FIG. 2. Mapa Geológico-Tectónico simplificado de Bolivia, mostrando las Provincias Geológicas y principales rasgos tectónicos (basado en Minaya et al., 1985).

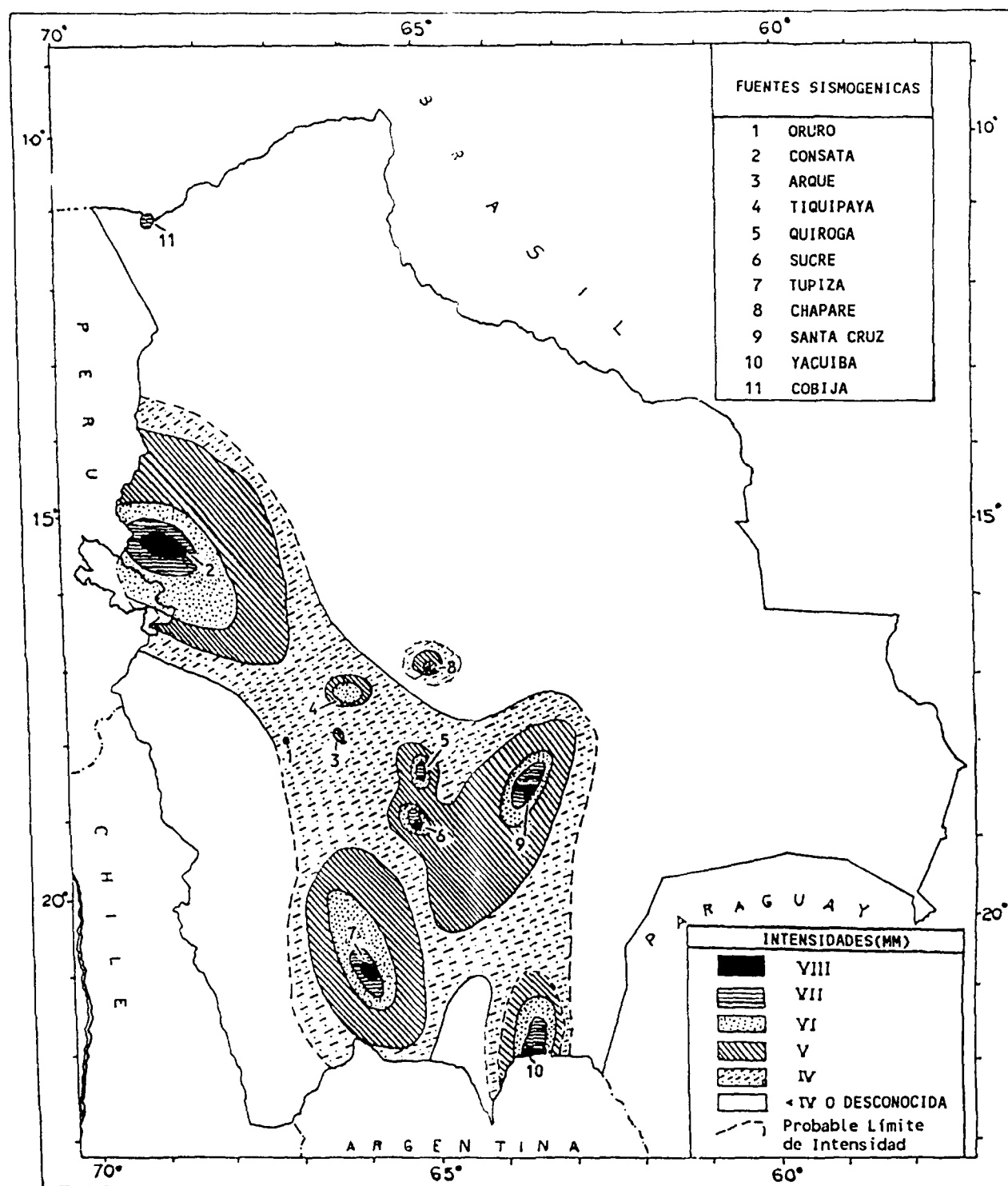


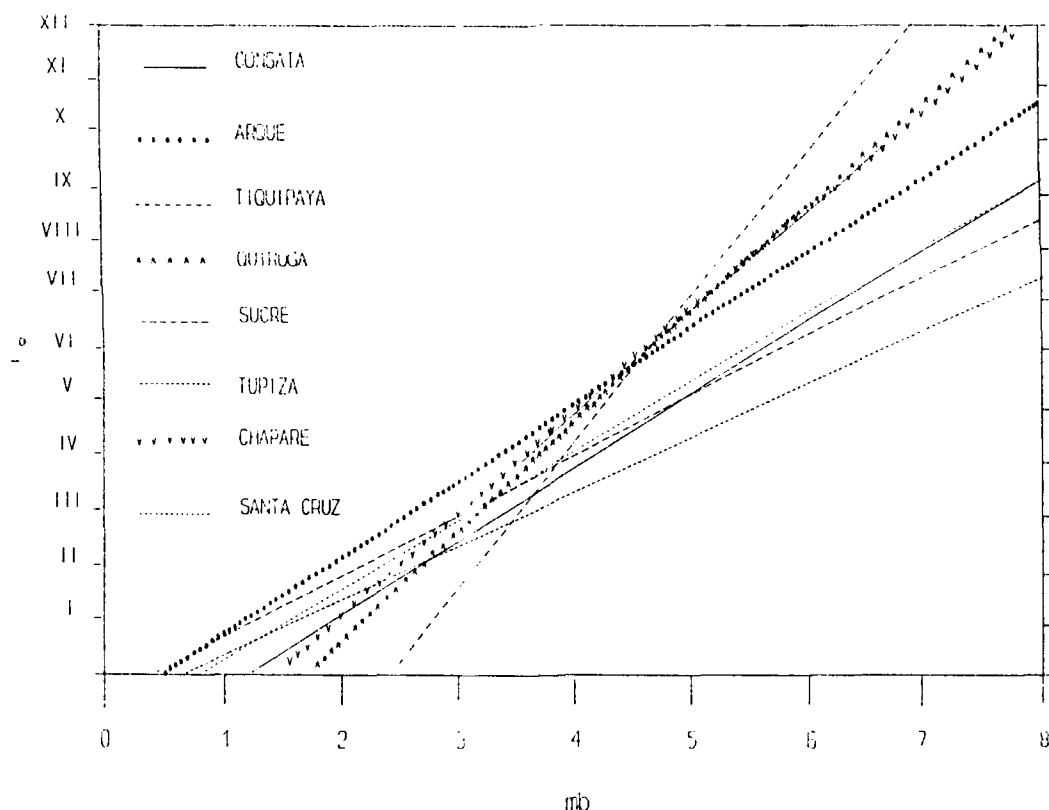
FIG. 3. Mapa de Areas de Máximas Intensidades Observadas en Bolivia (basado en Minaya, 1983) mostrando las fuentes sismogénicas asociadas con los mayores sismos.

TABLA 2

FUENTES SISMOGENICAS DE BOLIVIA RELACIONADAS CON LOS MAYORES SISMS

NUMERO	ZONA	LOCALIDAD DEL AREA DE EPICENTROS	PROVINCIA GEOLOGICA		DEPARTAMENTO
1	ORURO	Ciudad de Oruro	Altiplano	(norte)	ORURO
2	CONSATA	Consata	Cordillera Oriental	(norte)	LA PAZ
3	ARQUE	Arque	Cordillera Oriental	(centro)	COCHABAMBA
4	TIQUIPAYA	Tiquipaya y ciudad de Cochabamba	Cordillera Oriental	(centro)	COCHABAMBA
5	QUIROGA	Quiroga	Cordillera Oriental	(centro)	COCHABAMBA
6	SUCRE	Sucre, Yotala, Tarabuco	Cordillera Oriental	(centro)	CHUQUISACA
7	TUPIZA	Tupiza	Cordillera Oriental	(sur)	POTOSI
8	CHAPARE	Provincia Chapare	Subandino	(centro)	COCHABAMBA
9	SANTA CRUZ	Postrevall y Santa Cruz de la Sierra	Subandino-Llanuras Chaco-Benianas	(sur)	SANTA CRUZ
10	YACUIBA	Yacuiba	Subandino	(sur)	TARIJA
11	COBIJA	Cobija	Llanuras Chaco-Benianas	(norte)	PANDO

En las zonas de Cobija y Oruro no hay suficientes datos macrosísmicos porque los pocos sismos que se dan son locales (Tabla 2). Considerando cada fuente sismogénica y usando la ecuación (3) fueron calculadas las curvas generales de atenuación de las intensidades con la distancia hipocentral (ver Tabla 3).

FIG. 4. Relaciones entre  $I_o$  y  $m_b$  para las diferentes fuentes sismogénicas de Bolivia.

La Figura 4 muestra las relaciones calculadas empleando la fórmula (4) entre la máxima intensidad  $I_o$  y la magnitud  $m_b$  para cada fuente sismogénica; para Yacuiba fue asumida la misma relación de Sucre, porque tienen similar atenuación. Analizando la Figura 4, se observa que las fuentes que generan las mayores intensidades de sitio con relación a  $m_b$  son: Tiquipaya, Quiroga, Chapare y Arque, mientras que la menor es Tupiza; en general las relaciones de Consata, Santa Cruz y Sucre son aproximadamente iguales.

Aplicando la ecuación (5) las curvas de atenuación de las intensidades sísmicas con la distancia hipocentral fueron calculadas para diferentes magnitudes mb y fuentes sismogénicas de Bolivia (Fig. 5).

La Tabla 3 muestra las relaciones de atenuación sísmica calculadas para las diferentes fuentes sismogénicas consideradas, rango de profundidad y sus desviaciones standard, como también las relaciones calculadas por Minaya (1985) para Cochabamba, donde se aprecian diferencias en los resultados debido a que en este estudio se utilizaron más datos.

TABLA 3

RELACIONES DE ATENUACION SISMICA PARA BOLIVIA

FUENTE SISMOGENICA	RELACIONES DE ATENUACION	PROFUNDIDAD h	DESVIACION STANDARD
CONSATA	$I(D) = I_0 + 1.97 - 0.93 \log_{10} D - 0.013 D$		0.11
	$I_0 = 1.37 \text{ mb} - 1.64$	$h \geq 20 \text{ km}$	0.14
	$I(D) = 1.37 \text{ mb} + 0.33 - 0.93 \log_{10} D - 0.013 D$		0.10
ARQUE	$I(D) = I_0 + 6.3 - 1.28 \log_{10} D - 0.11 D$		0.10
	$I_0 = 1.28 \text{ mb} - 0.70$	$h \geq 30 \text{ km}$	0.25
	$I(D) = 1.28 \text{ mb} + 5.30 - 1.28 \log_{10} D - 0.11 D$		0.18
	* $I_0 = 0.89 \text{ mb} + 1.03$		* 0.79
TIQUIPAYA	* $I(D) = 0.88 \text{ mb} + 2.62 - 3.25 \log_{10} D - 0.0072 D$		
	$I(D) = I_0 + 5.49 - 2.72 \log_{10} D - 0.026 D$		0.07
	$I_0 = 2.36 \text{ mb} - 5.47$	$h \geq 30 \text{ km}$	0.30
	$I(D) = 2.36 \text{ mb} + 0.02 - 2.72 \log_{10} D - 0.026 D$		0.12
QUIROGA	* $I_0 = 1.23 \text{ mb} - 0.83$		* 0.78
	* $I(D) = 1.23 \text{ mb} + 2.77 - 3.0 \log_{10} D - 0.02 D$		
	$I(D) = I_0 + 13.0 - 8.16 \log_{10} D - 0.008 D$		0.18
	$I_0 = 1.94 \text{ mb} - 3.49$	$h \geq 35 \text{ km}$	0.19
SUCRE	$I(D) = 1.94 \text{ mb} + 9.51 - 8.16 \log_{10} D - 0.008 D$		0.17
	$I(D) = I_0 + 3.55 - 3.15 \log_{10} D - 0.015 D$		0.08
	$I_0 = 1.14 \text{ mb} - 0.23$	$h > 10 \text{ km}$	0.42
TUPIZA	$I(D) = 1.14 \text{ mb} + 3.32 - 3.15 \log_{10} D - 0.015 D$		0.11
	$I(D) = I_0 + 6.78 - 0.55 \log_{10} D - 0.029 D$		0.19
	$I_0 = 1.05 \text{ mb} - 0.70$	$h \geq 200 \text{ km}$	0.35
CHAPARE	$I(D) = 1.05 \text{ mb} + 6.08 - 0.55 \log_{10} D - 0.029 D$		0.18
	$I(D) = I_0 + 15.1 - 9.41 \log_{10} D - 0.025 D$		0.10
	$I_0 = 1.83 \text{ mb} - 2.90$	$h \geq 30 \text{ km}$	0.18
	$I(D) = 1.83 \text{ mb} + 12.2 - 9.41 \log_{10} D - 0.025 D$		0.11
SANTA CRUZ	* $I_0 = 1.16 \text{ mb} + 0.33$		* 0.48
	* $I(D) = 1.14 \text{ mb} + 1.14 - 1.21 \log_{10} D - 0.057 D$		
	$I(D) = I_0 + 1.68 - 0.99 \log_{10} D - 0.014 D$		0.13
	$I_0 = 1.27 \text{ mb} - 0.91$	$h \geq 10 \text{ km}$	0.37
YACUIBA	$I(D) = 1.27 \text{ mb} + 0.77 - 0.99 \log_{10} D - 0.014 D$		0.10
	$I(D) = I_0 + 0.36 - 0.6 \log_{10} D - 0.029 D$		0.12
	$I_0 = 1.14 \text{ mb} - 0.23$	$h > 0 \text{ km}$	0.42
	$I(D) = 1.14 \text{ mb} + 0.13 - 0.6 \log_{10} D - 0.029 D$		0.12

\* Minaya (1985)

En general se aprecia que la mayor atenuación de las intensidades sísmicas con la distancia sigue la dirección perpendicular a las estructuras geológico-tectónicas.

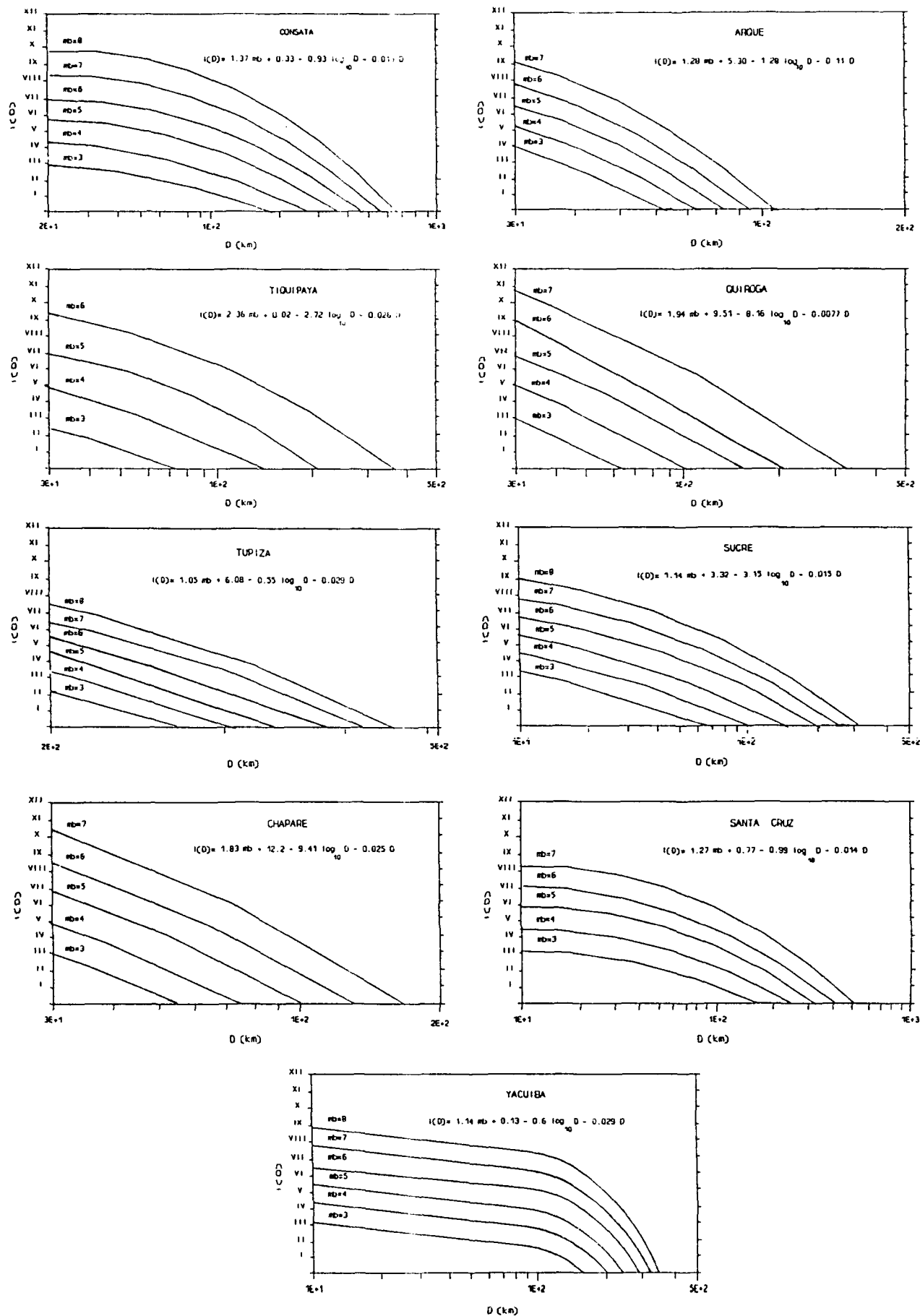


FIG. 5. Curvas de atenuación de las intensidades sísmicas  $I(D)$  con la distancia hipocentral ( $D$ ) para diferentes magnitudes  $m_b$  y fuentes sismogénicas de Bolivia.



Comparando las relaciones de atenuación sísmica para las diferentes fuentes sismogénicas de Bolivia (Fig. 6), se evidencia que están relacionadas a 4 tipos de estructuras geológico-tectónicas: Cordillera Oriental norte (Cordillera Real), Cordillera centro Oriental, Subandino central y sur, y Subandino-Llanuras Chaco Benianas. Los sismos de Arque y Chapare tienen la mayor atenuación, correspondientes a cuencas sedimentarias cuaternarias ubicadas en la Cordillera centro Oriental (Arque, Tiquipaya, Quiroga, Sucre, Tupiza), y las zonas del Subandino central (Chapare) y Subandino sur (Yacuiba).

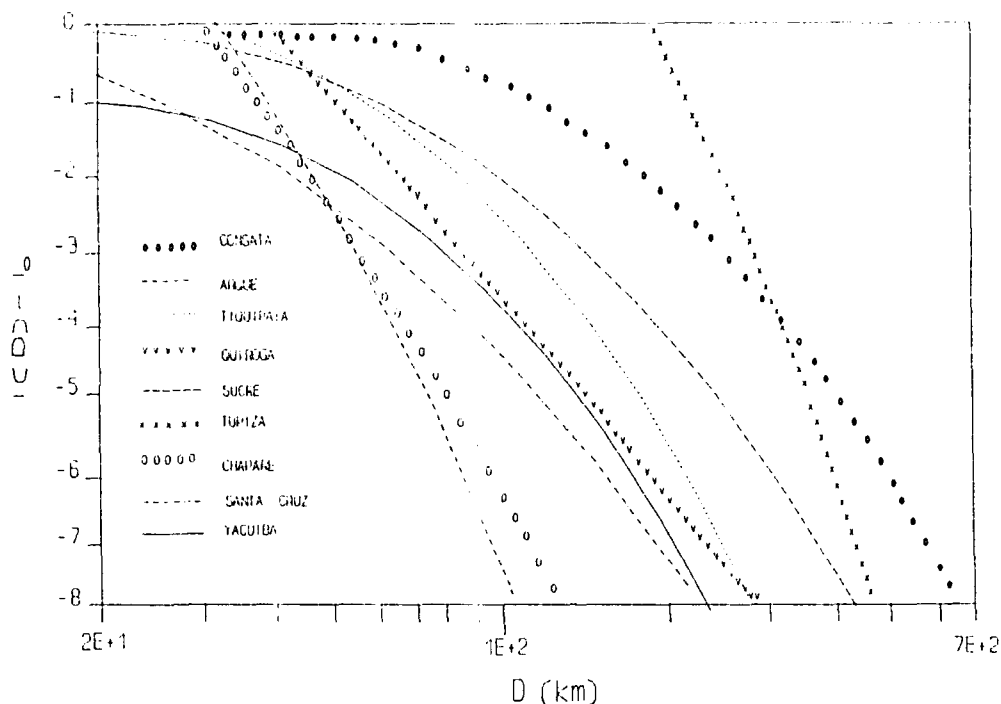


Fig. 6. Curvas de atenuación de las intensidades sísmicas con la distancia hipocentral para diferentes fuentes sismogénicas de Bolivia.

Los sismos de Sucre y Yacuiba presentan similar atenuación sísmica, los primeros relacionados con rocas paleozoicas de la Cordillera centro Oriental y los segundos al Subandino sur. Los sismos de Tupiza presentan una gran atenuación con la profundidad. Los sismos de Consata presentan la menor atenuación correspondiente a la Cordillera Oriental norte, seguidos por los de Santa Cruz, relacionados al Subandino central y a las Llanuras Chaco-Benianas.

#### AGRADECIMIENTOS

Agradezco a la Ing. Estela Minaya por sus comentarios, al Dr. Ramón Cabré S.J. por sus críticas revisiones y sugerencias a este manuscrito y al Lic. Hilarión Bilbao por sus comentarios en el tratamiento de datos. Este trabajo se realizó con los auspicios del Geophysics Laboratory, Air Force Systems Command, USAF, bajo el Grant AFOSR-89-0532 8.

## BIBLIOGRAFIA

- Ayala, R. (1990). Evaluación y Riesgo Sísmico en Bolivia. *Seminario Internacional de Microzonificación y Seguridad de Sistemas Públicos Vitales*, Lima. Perú.
- Cabré R., S.J. y A. Vega (1989). Sísmicidad de Bolivia, *Publicación No. 47, Observatorio San Calixto*, La Paz, Bolivia, 1989.
- CERESIS (1985). Catálogo de Terremotos para América del Sur: Bolivia, Brasil, Vol. 3, Lima, Perú.
- CERESIS (1984). Mapa de Intensidades para América del Sur, *Proyecto SISRA*.
- Chandra, U., J. G. Mc Whorter and Ali A. Nowroozi (1979). Attenuation of intensities in Iran. *Bull. Seism. Soc. Amer.*, 69, No. 1, 237-250.
- Descotes, P. M. y R. Cabré (1960). Historia Sísmica de Bolivia. *Boletín Inst. Bol. del Petróleo*, Vol. 5, No. 1-2, 16-18.
- Gupta and Nuttli (1976). Spatial attenuation of intensities for central United States earthquakes. *Bull. Seism. Soc. Amer.*, 66, 743-751.
- Gutenberg, B. and C. F. Richter (1955). Earthquakes magnitude, intensity, energy and acceleration (second paper). *Bull. Seism. Soc. Amer.*, 40, 105-145.
- Howell, B. F. (1974). Seismic regionalization in North America based on Average Regional Seismic Hazard Index. *Bull. Seism. Soc. Amer.*, 64, 1509-1528.
- Howell, B.F. and T. R. Schultz (1975). Attenuation of MM intensity with distance from epicenter. *Bull. Seism. Soc. Amer.*, 65, 651-665.
- International Seismological Centre, Regional Catalogues of Earthquakes, Newbury, Berkshire, United Kingdom, 1970-1989.
- Karnik, V. (1969). Seismicity of the European area, Part I, Reidel, Amsterdam, 364pp.
- Minaya, E., Claire, H. and Vega, A. (1983). Mapa Sismotectónico de Bolivia, *Proyecto SISRA*, 1983.
- Minaya, E. (1983). Mapa de Areas de Máximas Intensidades Observadas, *Proyecto SISRA*.
- Minaya, E. (1985). Atenuación de la intensidad en la región de Cochabamba, *Simposio sobre el Peligro y Riesgo Sísmico y Volcánico en América del Sur, San Juan, Argentina, CERESIS*, 103-115, 1984.
- Montes de Oca, I. (1989). Geografía y Recursos Naturales de Bolivia, *Editorial Educacional*, La Paz, Bolivia, 1989.
- Ocola, L. (1982). Catálogo de Sismos - República de Bolivia, *Proyecto SISAN*.